NSW STATE EMERGENCY SERVICE

NSW Tsunami Inundation Modelling and Risk Assessment

Document Control:						
Version	Status	Date	Author		Reviewer	
			Name	Initials	Name	Initials
1	Interim Draft	17 March 2011	S.J. Garber / C.J. Beadle	SJG / CJB	L.C. Collier / P.D. Treloar	LCC / PDT
2	Revised Draft	28 September 2011	S.J. Garber / C.J. Beadle	SJG / CJB	P.D. Treloar	PDT
3	Final Draft	4 May 2012	S.J. Garber / C.J. Beadle	SJG / CJB	P.D. Treloar	PDT
4	Final	22 July 2013	C.J. Beadle	CJB	P.D. Treloar	PDT

Prepared for NSW State Emergency Service and the Office of Environment and Heritage with funding from the National Disaster Mitigation Program

By Cardno (NSW/ACT) Pty Ltd

ABN 95 001145 035

EXECUTIVE SUMMARY

New South Wales is a coastally-oriented state with a large percentage of the population using coastal areas for residential, commercial and recreational purposes. With over 1300km of coastline, NSW is exposed to tsunami originating from a range of possible sources. The NSW Tsunami Risk Assessment was borne from a need to better understand tsunami risk in order to underpin detailed emergency response planning as part of the *NSW Tsunami Emergency Sub Plan* (a sub plan of the *NSW State Disaster Plan;* NSW SES, 2008). This study forms Stage 2 of the NSW Tsunami Risk Assessment, and has involved the detailed inundation modelling and exposure assessment of vulnerable low-lying coastal areas.

This report has been prepared under grant funding from the Attorney-General's Department Natural Disaster Mitigation Program by Cardno Coastal & Ocean for both the NSW Office of Environment and Heritage and the NSW State Emergency Service. The report describes detailed tsunami inundation modelling, deterministic hazard mapping and exposure assessments for five specific sites along the NSW coast, all identified during Stage 1 as being potentially more vulnerable to tsunami.

The five coastal locations include:-

- Swansea/Lake Macquarie;
- Manly;
- Botany Bay/Cronulla/Kurnell;
- Wollongong/Port Kembla; and
- Merimbula.

The overall objective of the Stage 2 project was to identify and outline areas of 'high hazard' resulting from potential major tsunami events along the NSW coastline. This will allow for an improved understanding of the tsunami risk to the NSW coastline, enabling future consideration of tsunami impacts in coastal zone management and planning and assist in the development of tsunami emergency planning, response and community education. Furthermore this study has attempted to expand the current understanding of nearshore tsunami behaviour, specifically how it is affected by variables such as source zone location, initial rupture magnitude as well as the impact of coastline types.

NSW is exposed to tsunami originating from a range of possible sources, with those generated by earthquakes account for approximately 75% of all tsunami, globally. NSW has over 1300km of coastline and is exposed to numerous tsunamigenic sources including subduction zones that border the Pacific Ocean basin, located in the South Pacific, Southeast Asia, Japan, the Aleutian Islands, as well as the west coasts of North, Central and South America. Otherwise known as the 'Pacific Ring of Fire' this highly active seismic zone spans 40,000km, borders four continents and is made up of volcanoes, earthquakes, deep sea trenches and major fault zones. Furthermore, subduction zones in the Pacific Ocean are known to have produced major historical tsunami and are considered the most likely source of future events.

Therefore, this assessment only considers tsunami generated by earthquakes along subduction zones. This is in keeping with the findings of the Stage 1 Assessment, which found that subduction zone earthquakes are the most likely source of significant tsunami to the NSW coastline.

Inundation modelling was completed using the Delft3D hydrodynamic modelling system, which has been extensively used and tested to model tsunami events worldwide. Site specific data of tsunami inundation along the New South Wales coastline was not available to undertake direct numerical model verification for this study. However a number of actual subduction zone earthquake events were identified that resulted in observable, albeit small, tsunami responses at the study sites (measured by high resolution tide gauges). This enabled verification of the model setup to ensure that the correct nearshore response, in terms of tsunami amplification and frequency oscillations, was being produced by the model.

Furthermore, to overcome the lack of site-specific field data of overland inundation a series of 'benchmark' events were assessed in order to validate the Delft3D model. Referred to as 'benchmark verification' this process provides confidence that the numerical scheme and model setup utilised performs to an industry standard. In both the benchmark verification and site-specific verification, the Delft3D models were shown to perform well and with a suitable level of accuracy to be applied to the NSW Tsunami Risk Assessment.

Five individual models were established for each of the study sites. The extent and size of the individual study area grids vary depending on site specific features such as landforms (headlands and embayments) and the topographic lie of the land.

A range of data has been utilised to inform and undertake these investigations, including inputs for the development of the numerical models used in this study. Of key importance to this study was the use of two separate tsunami databases that were accessed to provide data on tsunami source, magnitude and probability for this assessment. They were the GA Tsunami Data Access Tool (Tsu-DAT) and the BoM Enhanced Tsunami Scenario Database: T2 (T2 Database). Both databases contain a population of synthetic, hypothetical tsunami events that are based on the current understanding of subduction zone dimensions and seismic activity.

The two databases were drawn upon to allow for both an initial identification of the tsunami risk and to consider individual events as well as draw upon tsunami time-series data for use as boundary conditions for the inundation modelling. Recurrence interval estimates identified within this study are based on the recurrence intervals presented in Tsu-DAT. As such, the resulting inundation from a given ARI tsunami, reported in Tsu-DAT in 100m water depth, does not lead necessarily to the equivalent ARI inundation extent due to the complex behaviour of tsunami in the nearshore region. To account for this within the current study a series of model runs was completed at each recurrence level to assess a range of tsunamigenic sources, this ensures that any localised sensitivities at the study sites are included in the investigation thereby providing a better estimate of the inundation at each recurrence level. As such, the average recurrence intervals presented can be considered a best estimate only.

In total, 24 scenarios were assessed for each study site and detailed output from the inundation modelling provided for hydraulic parameters including peak water level, peak inundation depth, extent of inundation, peak velocity and hydraulic hazard (V x D). In addition the duration of inundation is presented. It is intended that this output from the inundation modelling, provided as high resolution GIS layers, can be used in future detailed risk assessments.

The nature of the inundation at each study site is dependent on the topography of nearshore and foreshore areas, however a qualitative assessment of the model outputs suggests that the threshold for significant inundation is between the 1000 and 2000-years ARI levels for four of the study sites, while for Manly this threshold is between the 500 and 1000-years ARI levels. These outcomes are consistent with the existing Joint Australian Tsunami Warning Centre system, which found similar thresholds for the issuance of land warnings at the five study sites.

This project has been overseen by the *Tsunami Inundation Modelling and Risk Assessment Steering Committee* (Steering Group). The Steering Group consisted of representatives from the NSW SES, OEH, Bureau of Meteorology (BoM), Geoscience Australia (GA) and Cardno Coastal & Ocean. The committee was involved in defining the scope of work, development of the approach and methodology and discussion of key issues and outcomes.

TABLE OF CONTENTS

TABLES

FIGURES

APPENDICES

GLOSSARY AND ABBREVIATIONS

Australian Height Datum (AHD)	A common national plane of level corresponding approximately to mean sea level.
ARI	Average Recurrence Interval; relates to the probability of occurrence of a design event.
BoM	Bureau of Meteorology.
Calibration	The process by which the results of a computer model are brought to agreement with observed data.
CAWCR	The Centre for Australia Weather and Climate Research. A partnership between the CSIRO and the Bureau of Meteorology.
Coastal Inundation	Flooding of coastal land due to inundation by ocean waters.
CSIRO	The Commonwealth Scientific and Industrial Research Organization.
DART	Deep ocean Assessment and Report of Tsunami
DEM	Digital Elevation Model.
Discharge	The rate of flow of water measured in terms of volume per unit time. It is to be distinguished from speed or velocity of flow, which is a measure of how fast the water is moving rather than how much is flowing.
Ebb Tide	The outgoing tidal movement of water within an estuary.
Eddies	Large, approximately circular, swirling movements of water, often metres of tens of metres across. Eddies are caused by shear between the flow and a boundary or by flow separation from a boundary.
Estuarine Processes	The processes that affect the physical, chemical and biological behaviour of an estuary, e.g. Predation, water movement, sediment movement, water quality etc.
Estuary	An enclosed or semi-enclosed body of water having an open or intermittently open connection to coastal waters and in which water levels vary in a periodic fashion in response to ocean tides.
Flood Tide	The incoming tidal movement of water within an estuary.
Foreshore	The area of shore between low and high tide marks and land adjacent thereto.
GA	Geoscience Australia.
GIS	Geographical Information System.
GURAS	Geo-coded Urban and Rural Addressing System.
Habitable Land	Land currently containing residential, recreational, commercial or industrial development.

HAT	Highest Astronomical Tide.
Hazard	Hazard is a source of potential harm or a situation with a potential to cause loss.
Hydraulic Hazard	Refers to the hazard caused by flowing water and is a product of the depth and velocity.
Intertidal	Pertaining to those areas of land covered by water at high tide, but exposed at low tide, e.g. Intertidal habitat.
Inundation	The flooding of normally dry land due to an increase in ocean water levels.
JATWC	The Joint Australian Tsunami Warning Centre
LAT	Low Astronomical Tide.
LEP	Local Environment Plan.
LGA	Local Government Area.
LiDAR	(*Li*ght *D*etection *A*nd *R*anging) is an optical remote sensing technology that measures properties of scattered light to find range and/or other information of a distant target.
LPI	Land and Property Information NSW. A division of the Department of Finance & Services, it is the key provider of land information services in New South Wales.
Mathematical Models	An analytical representation of a physical, chemical or biological process of interest.
MHWM	Mean High Water Mark.
MHWN	Mean High Water Neap.
MHWS	Mean High Water Springs.
MLWN	Mean Low Water Neap.
MLWS	Mean Low Water Springs.
MSL	Mean Sea Level.
Neap Tides	Tides with the smallest range in a monthly cycle. Neap tides occur when the sun and moon lie at right angles relative to the earth (the gravitational effects of the moon and sun act in opposition on the ocean).
NPW Act	NSW *National Parks and Wildlife Act 1974.*
NSW	New South Wales.
NSW SES	The New South Wales State Emergency Service.
Numerical/ Computer Model	The discretisation of mathematical models to enable the solution of complex mathematical relationships. Computers are often required to solve the underlying equations in the spatial and temporal scales

	required for process investigations. In this report, the models referred to are mainly involved with wave and current processes.
OEH	NSW Office of Environment and Heritage
Phase Lag	Difference in time of the occurrence between high (or low) water and maximum flood (or ebb) velocity at some point in an estuary or sea area.
PKPC	Port Kembla Port Corporation
Salinity	The total mass of dissolved salts per unit mass of water. Seawater has a salinity of about 35g/kg or 35 parts per thousand.
SEPP	State Environment Planning Policy.
SLR	Sea Level Rise.
Spring Tides	Tides with the greatest range in a monthly cycle, which occurs when the sun, moon and earth are in alignment (the gravitational effects of the moon and sun act in concert on the ocean).
Tidal Lag	The delay between the state of the tide at the estuary mouth (e.g. high water slack) and the same state of tide at an upstream location.
Tidal Propagation	The movement of the tidal wave into and out of an estuary.
Tides	The regular rise and fall in sea level in response to the gravitational attraction of the Sun, Moon and Earth.
Tributary	Catchment, stream or river which flows into a larger river, lake or water body.
Tsunamigenic	Refers to the ability of an object or area to generate a tsunami.
Wave Height	The height of the tsunami wave crest above the still water level, i.e. excluding tide (IOC-UNESCO, 1998). As opposed to the coastal engineering definition of wave height, being the height between a wave crest and trough. When referring to a particular tsunami event, the wave height refers to the largest wave height in the tsunami wave train.
Wave Length	The distance between two wave crests.
Wave Period	The time it takes for two successive wave crests to pass a given point.
Wave Run-up	The vertical distance between the maximum height that a wave runs up the beach (or a coastal structure) and the still water level, comprising tide and storm surge.
Wave Set-up	Wave set-up in included implicitly in wave run-up calculations.

1 INTRODUCTION

The wide-spread loss of lives and damage in South-East Asia from the Boxing Day tsunami of 2004 was a stark reminder of the potential devastation caused by tsunami. Since that time, the importance of a functional tsunami emergency management system has been prioritised in many jurisdictions, and thus increasing understanding of the tsunami risk in Australia has been on the national risk assessment agenda.

1.1 Background

The NSW Tsunami Risk Assessment was borne from a need to better understand tsunami risk in order to underpin detailed emergency response planning as part of the *NSW Tsunami Emergency Sub Plan* (a sub plan of the *NSW State Disaster Plan;* NSW SES, 2008). Under the *State Disaster Plan* and the *State Emergency Services Act*, 1989, the State Emergency Service (NSW SES) is responsible for the preparing for and responding to tsunami.

The NSW Tsunami Risk Assessment has been completed in two stages. Stage 1 was a broad-based risk assessment of the entire NSW coast (discussed in Somerville et. al., 2009; *Risk Frontiers and URS Corporation, 2008*), with Stage 2 (this report) comprising of detailed inundation modelling and risk assessment of areas highlighted in Stage 1 as being potentially more vulnerable to tsunami. In support of Stage 2 of the NSW Tsunami Risk Assessment, Geoscience Australia has carried out tsunami inundation modelling around Batemans Bay and Gosford – but these sites were not included in Cardno's brief.

This report has been prepared with grant funding from the Attorney-General's Department Natural Disaster Mitigation Program by Cardno Coastal & Ocean for both the NSW Office of Environment and Heritage (OEH) and the NSW SES. The report describes detailed tsunami inundation modelling, deterministic hazard mapping and risk assessments for specific sites along the NSW coast.

1.2 The Study Area

While this report forms part of the overall tsunami risk assessment along the NSW coast, five coastal locations have been specifically investigated as part of this assessment. These five study areas, shown in Figure 1.1, were identified in Stage 1 of the NSW Tsunami Risk Assessment (*Risk Frontiers and URS Corporation, 2008*) as being potentially more vulnerable than other locations in NSW to tsunami inundation and were therefore selected for detailed hydrodynamic modelling to provide detailed information on the likely inundation associated with tsunami. The five coastal locations include:-

- Swansea/Lake Macquarie (see Figure 1.2);
- Manly (see Figure 1.3);
- Botany Bay/Cronulla/Kurnell (see Figure 1.4);
- Wollongong/Port Kembla (see Figure 1.5); and
- Merimbula (see Figure 1.6).

The extent of each study area is defined by local geomorphic features, such as headlands and embayments, and as far landward so as to define the full extent of expected tsunami inundation. This was nominally

defined as the area up to the 15mAHD contour.

1.3 Project Objectives

The overall objective of this project is to identify and outline areas of 'high hazard' resulting from potential major tsunami events along the NSW coastline. This will allow for an improved understanding of the tsunami risk to the NSW coastline, enabling future consideration of tsunami impacts in coastal zone management and planning and assist in the development of tsunami emergency planning, response and community education. Furthermore this study aims to expand the current understanding of nearshore tsunami behaviour, specifically how it is affected by variables such as source zone location, initial rupture magnitude as well as the impact of coastline types.

1.4 Project Steering Committee

This project has been overseen by the *Tsunami Inundation Modelling and Risk Assessment Steering Committee* (Steering Group). The Steering Group consisted of representatives from the NSW SES, OEH, Bureau of Meteorology (BoM), Geoscience Australia (GA) and Cardno Coastal & Ocean. The committee was involved in defining the scope of work, development of the approach and methodology and discussion of key issues and outcomes.

2 UNDERSTANDING TSUNAMI

Tsunami is a Japanese word; “tsu” meaning harbour and “nami” meaning wave. A tsunami generally consists of a series of propagating long waves (called a tsunami wave train) that that can travel trans-oceanic distances. In the past, tsunami have often been referred to incorrectly as "tidal waves". Tides are the result of gravitational influences of the Moon, Sun, and the Earth. Tsunami are not caused by the tides and are unrelated to the tides; although the behaviour of a tsunami striking a coastal area is influenced by the tide level at the time of impact. Tsunami travel across the open ocean at great speeds and can build into large, devastating waves in shallow water near the shoreline and then propagate into the onshore area.

Due to the immense volumes of water and energy involved, tsunami can devastate coastal regions, as exemplified by the 2004 Boxing Day tsunami, where, according to the U.S. Geological Survey over 230,000 people from 14 different countries perished and millions more were displaced.

2.1 Causes of Tsunami

Tsunami are caused by the sudden displacement of a large volume of water. This displacement may be caused by sudden movement of the ocean due to (Geoscience Australia, 2010a):

- Earthquakes (75%);
- Landslides (by both land to sea and on the sea floor (8%);
- Large volcanic eruptions (5%), and
- The impact of a large meteorite in the open ocean (2%).

These sources of tsunami are referred to as ‘tsunamigenic sources’. 10% of all tsunami have no identifiable source (Geoscience Australia, 2010a). One such source is from meteorological events, known as Rissaga, where large and sudden variations in atmospheric pressure can generate long wave events that result in tsunami-like impacts at the coast.

Most tsunami are caused by earthquakes generated in a ‘subduction zone’, an area where a tectonic plate is being forced down into the mantle by plate tectonic forces. Here one plate (the subducting plate) attempts to slide underneath an adjacent plate (the overriding plate). In a subduction zone the friction force between the subducting plate and the overriding plate is vast. This friction prevents a slow and steady rate of subduction and instead the two plates become "stuck".

Over time, the subduction plate continues to descend into the mantle. As the two plates are essentially stuck together, this motion causes the overriding plate to slowly bend and distort. The result is an accumulation of energy very similar to the energy stored in a compressed spring. Energy can accumulate in the overriding plate over long periods of time that can span decades or even centuries. Energy accumulates in the overriding plate until it exceeds the frictional forces between the two stuck plates. When this happens, the overriding plate snaps back into an unrestrained position. The incredible force of the Earth’s plate shooting upwards creates a huge displacement in the overlying water level.

Tsunami generated by earthquakes account for approximately 75% of all tsunami. Furthermore, because the

vertical displacements and rupture lengths of earthquakes can be estimated by scientists, it is possible to generate approximate surface wave time-series for these tsunami. Earthquakes are complicated phenomena and the seabed plate motion needs to be simplified in those analyses.

Therefore, this assessment only covers tsunami generated by earthquakes along subduction zones. This is in keeping with the findings of the *Risk Frontiers and URS Corporation, (2008)*, which found that subduction zone earthquakes are the most likely source of significant tsunami to the NSW coastline.

Only a very small proportion of tsunami are caused by landslides and account for about 8% of all tsunami. Waves generated by landslides occur when an unstable rock slope fails and the debris enters a body of water. As masses of rock or soil move underwater or slide down into a body of water, a series of long waves is formed that will travel without loss of significant energy from the point of generation to opposite shores (Kamphuis, 2010). However, the majority of landslide-induced tsunami occur in lakes and reservoirs, where steep slopes surround large bodies of water, although submarine landslides, particularly around areas of continental shelf have been known to trigger tsunami also. Whilst it is possible to model tsunami wave time series resulting from landslides, it is near impossible to associate probabilities with these events and so tsunami resulting from landslides are not included in this assessment.

Volcanoes can generate tsunami in a number of ways. A submarine or offshore volcanic eruption can produce a high magnitude lift on the seafloor, which pushes water upwards to generate tsunami. Similarly tsunami can be generated by pyroclastic flows impacting on water and avalanches of cold rock, where the failure of a submarine volcano's slope results in the sudden disturbance of water, creating tsunami waves. While volcanic eruptions are responsible for approximately 5% of all tsunami, the form and extent of volcanically-produced tsunami are almost impossible to predict and as such have also been excluded from this assessment.

Meteorite impacts are extremely rare and account for only 2% of all tsunami events.

2.2 Long Wave Propagation

When an earthquake occurs below or adjacent to a body of water, the sudden movement of the landmass at first generates confused motion in the water, but after a relatively short distance a wave train of the order of 2 - 10 long-period waves is generated and radiates outwards from the epicentre of the quake.

Since there is little friction in deep oceans the waves preserve much of their energy as they travel over long distances, but since the waves radiate from a single location (much like when a pebble is dropped into water), the energy density, and therefore wave heights will decrease with propagation distance from the epicentre.

Tsunami waves in the deep ocean usually possess a wavelength of approximately 10 to 500 km. Because of these large wave lengths, their speed of propagation generally follows shallow water wave theory, where wave speeds are given by the formula:-

$$c = \sqrt{gd}$$

where:

c = the wave speed
g = acceleration due to gravity (9.81m/s^2)
d = water depth (m)

As deep ocean water depths are typically 4000 to 5000 m, such waves can travel at speeds up to 800 km/hour; hence they can cover trans-oceanic distances in a matter of hours. However, due to these enormous wavelengths tsunami waves generally possess periods in the vicinity of 10 to 30 minutes and amplitudes, in deep water, typically smaller than 1m. Whilst DART buoys can detect a tsunami a few cm high, they are not often observed or felt by boats in deep water and it is common for ships out to sea to not notice their passage.

2.3 Nearshore Behaviour of Tsunami

The danger of tsunami lies not in deep water, but rather when they come ashore. As a tsunami leaves the deep water of the open ocean and arrives at shallow waters near the coast, it undergoes a major transformation. As defined in Section 2.2, the speed of tsunami waves are related to the depth of water in which they travel. Hence, as a tsunami leaves the deep water of the open ocean and travels into the shallower water near the coast, it will slow down.

Furthermore, as a tsunami wave propagates into shallow water the period of the wave remains the same, and thus more water is forced between the wave crests causing the heights of the wave to increase and the wavelengths to decrease (conservation of wave energy flux). This is known as 'wave shoaling', and because of this shoaling effect, a tsunami that was imperceptible in deep water may grow to have wave heights of several metres or more near the coast, but travels more slowly.

Additionally reefs, headlands, bays, entrances to rivers, undersea features and the slope of the seabed also cause modification of tsunami waves as they approach the shoreline. Depending on whether the first part of the tsunami to reach the shore is a crest or a trough, it may appear as a rapidly rising or falling tide. If the trough of the tsunami wave reaches the coast first, this causes a phenomenon called drawback, where the water level recedes significantly in order to supply the volume of water for the wave that follows. This drawback can exceed hundreds of metres and is followed several minutes later by a near-vertical wall of water propagating in from the sea as the leading wave breaks and approaches the shoreline.

When the crest of the wave propagates onto land the resulting temporary rise in sea level is called 'run-up' (usually expressed in metres above a reference datum). The momentum and energy in this moving wall of water (potentially up to several metres high) damages or destroys most things in its path, before minutes later rushing back out to sea. A large tsunami will have multiple waves arriving over a period of hours, with significant time between the wave crests, usually 10 to 30 minutes (Kamphuis, 2010). The first wave to reach the shoreline may not have the highest run up.

The destruction by tsunami run-up is often complete, as most areas are swept over by several incoming and receding waves. The flooding of an area can extend kilometres inland, covering large areas of land with water and debris; depending upon the character of the land and hinterland levels.

Most tsunami do not result in significant run-up and overland inundation (particularly along the NSW coast),

however, even small amplitude events typically result in significant currents when the shallow water waves travel into constricted entrances, coastal embayments as well as ports and harbours. These currents can have significant impacts upon swimmers, marine craft and even maritime infrastructure.

Figure 2.1 provides an illustration that describes how a tsunami travels from deep water to cause inundation of low-lying coastal areas.

2.4 Vulnerability of the NSW Coastline to Tsunami

Like the rest of Australia, New South Wales is a coastally-oriented state with a large percentage of the population using coastal areas for residential, commercial and recreational purposes. The JATWC has defined areas at risk of tsunami as areas that are within 1km of the coast and less than 10m above mean sea level. The coastal zone of NSW (New South Wales State Emergency Service, 2005 and Surf Life Saving NSW, 2008 referenced in Beccari and Davies, 2009) has:-

- A population of 328,800 (5.2% of the State's population). It should be noted that this population grows significantly during the summer holiday period.
- 160,700 dwellings.
- 225 caravan parks and camping grounds.
- 308 educational and child care facilities.
- 9 hospitals.
- 56 aged care facilities.

NSW has over 1300km of coastline and is exposed to numerous tsunamigenic sources including subduction zones located in the South Pacific, Southeast Asia, Japan, the Aleutian Islands, as well as the west coasts of North, Central and South America.

2.4.1 Geological and Historical Tsunami Records in NSW

A vital step towards a proper understanding of the tsunami hazard on the NSW coastline is to investigate the history of tsunami in the area. Dominy-Howes (2007) created a catalogue of past tsunami affecting Australia. This catalogue was split into two distinct sections. The first being "palaeotsunami record", with the second being the "historical tsunami record". The former includes all estimated tsunami occurrences prior to European settlement (1788), and the latter includes all tsunami occurrences after European settlement. These palaeotsunamic records are derived from analyses of deposited sediments along the NSW coastline.

Unfortunately, due to the nature and type of evidence proposed for palaeotsunami, as well as the accuracy of the evidence and the possibility of erroneous interpretation, placing too much weight on the palaeotsunamic record should be avoided. The maximum reported run-up for a palaeotsunami is +100m AHD, potentially 130m. This interpreted event occurred at Jervis Bay approximately 8700-9000 years ago (Dominy-Howes, 2007). It is not known what processes generated this tsunami or where it came from, but it is important to note that the mean sea level was approximately 100m lower than the present day level. A tsunami that is reported to have occurred approximately 6500 years ago may have inundated to a distance of 10km inland across the Shoalhaven delta area of NSW. Again, no information is available about the cause or origin of this

event.

On the other hand, approximately 50 events have been recorded in Australia since 1788. According to Dominy-Howes (2007), more than 75% of all historic events in Australia between 1788 and 2006 affected NSW in some form. The majority of these tsunami have been barely noticeable, recorded only on tide gauges, with very little observed run-up. The most severe run-up recorded in NSW over this time period was +1.7m AHD, recorded at Eden on 23 May 1960 (Dominy-Howes, 2007). This was the result of a Mw 9.5 earthquake in Central Chile on 22 May 1960. It is interesting to note that for the same event, Dominy-Howes (2007) reports that run-up at Newcastle reached only 0.2m and 0.0m at Sydney. However, the Bureau of Meteorology (1998) and Beccari and Davies (2009) report this same incident producing a wave height of 0.8m at Sydney, but do not report a height at Eden. However, they do report considerable damage from Brisbane to Eden, being most severe at Sydney and Evans Head (most likely arising from strong currents in 'shallow water' port areas).

Other notable events that have affected NSW in this time period include the Chilean earthquake and tsunami on 14 August 1868, where a number of boats broke from their moorings in Newcastle and Sydney as well as in 1877, when a tsunami with its source in North Chile caused some tidal fluctuations and minor disturbances in Sydney and Newcastle. More recently the 2011 Japanese tsunami was recorded at a number of locations along the NSW coast (see Section 7.3), with an observed wave height of 0.37m at Eden (no reported land inundation).

2.4.2 Potential Sources of Tsunami for the NSW Coast

NSW is exposed to tsunami originating from a range of possible sources. As outlined in Section 2.4, there exist a number of subduction zones that border the Pacific Ocean basin. Otherwise known as the 'Pacific Ring of Fire' this highly active seismic zone spans 40,000km, borders four continents and is made up of volcanoes, earthquakes, deep sea trenches and major fault zones. However, it is considered that the most significant tsunami threat to the NSW coast would be from those originating along the various tectonic subduction zones on the edge of the Indo-Australian Plate, in the South West Pacific. These include the New Hebrides Trench, the Solomon Trenches, the Tonga-Kermadec Trench and the Puysegur Trench. Distant tsunami sources including Mid and South America, Cascadia, the Aleutian Islands and Japan also pose a tsunami risk to the NSW coast. In fact, since European settlement it is the Peru-Chile Trench that has generated the majority of the largest tsunami measured along the NSW coast (Beccari and Davies, 2009).

It is worth noting that another potential source for tsunami affecting the NSW coast are landslides off the continental shelf (Geoscience Australia, 2009).

In a probabilistic context, the potential number of source zones decreases as ARI increases. That is, there are many potential sources of 100yr ARI tsunami but only a few regional sources at higher ARI's such as 10,000yr ARI (Geoscience Australia, 2010b).

Figure 2.2 presents the major source zones that have been considered within this assessment.

3 SUPPORTING DATA

Cardno has been provided with a range of data from OEH and others to inform and undertake these investigations, including inputs for the development of the numerical models used in this study. These data are described herein.

3.1 Bathymetric and Topographic Data

The numerical models established for this study (Section 5) endeavor to simulate the propagation to and inundation of the selected study areas by tsunami from a range of sources. To establish the correct hydrodynamics within the inundation simulations detailed bathymetric and topographic information is required.

A Digital Elevation Model (DEM) was developed for each study area extending from approximately 50km north and south of each site out to the 2000mAHD depth (approximately 50km-70km offshore). The DEM was developed from a range of sources including:-

- LiDAR data provided by OEH
- Hydrographic survey data conducted at each site (collated from various sources and supplied by Manly Hydraulics Laboratory (MHL))
- 1km Digital Terrain Model of Australia/NZ (Whiteway, 2009)

The topographical LiDAR data generally possessed a horizontal resolution of 1m. In terms of vertical accuracy, a standard deviation of 0.15 metres (68% confidence) is the historical average for LiDAR obtained from historical benchmark data collected during previous surveys and during trials (Tenix, 2008).

3.2 Tidal Constants

Tidal water levels used to drive the regional oceanographic models were predicted using 10 offshore deep water tidal constants. Offshore tidal constants were extracted from the Oregon State University global model of ocean tides (TPXOv7.2) which uses track-averaged data from the satellites TOPEX/Poseidon and Jason (on TOPEX/POSEIDON tracks since 2002). The methodology of the global tide models is described in Egbert and Erofeeva (2002).

TPXOv7.2 provides up to 10 tidal constants on a 1/4 degree resolution full global grid. The tides are provided as complex amplitudes of earth-relative sea-surface elevation for eight primary (M_2, S_2, N_2, K_2, K_1, O_1, P_1, Q_1) and two higher order (M_4, MS_4) harmonic constituents.

Tidal constants at the local study sites were obtained from the *Australia National Tide Tables 2010*. Where required, these local constants were used to derive predicted tidal signals for model calibration.

3.3 Water Level Data

Recorded inshore water level data was provided by MHL and was used to assist in the tidal calibration of the Delft3D model covering the Merimbula area. The MHL data included water level data from both the Merimbula Lake, and Merimbula Wharf tide gauges. Predicted tides were used for this task all other study

sites.

Further tide gauge (and current meter) data was obtained from MHL and Port Authorities to identify and analyse historical tsunami events for model verification tasks. This data is detailed in Section 7.3.1.

3.4 Cadastral Information

In order to properly describe the flow of a tsunami over land it is necessary to have detailed information of the land usage and facility/services boundaries. To this extent, cadastral information was provided by OEH that allowed for the identification of roads and land parcels. Cadastral information from the following Local Government Areas were utilised:-

- Bega Valley Shire Council;
- Hurstville Council;
- Kogarah Council;
- Lake Macquarie City Council;
- Manly Council;
- Rockdale Council;
- Randwick Council;
- Sutherland Shire Council; and
- Wollongong City Council.

Additionally, information for these council zones was provided from the Geo-coded Urban and Rural Addressing System (GURAS) database (provided by LPI). This database uniquely locates addresses with a real world position (latitude and longitude), and describes multi-dwelling properties in a way that a simple cadastral information cannot. This data was used in the Risk Assessment in Section 9.

3.5 Tsunami Scenario Databases

Two separate tsunami databases were accessed to provide tsunami data for this assessment. They were the GA Tsunami Data Access Tool (Tsu-DAT) and the BoM Enhanced Tsunami Scenario Database: T2 (T2 Database).

The two databases were drawn upon to allow for both an initial identification of the tsunami risk and to consider individual events as well as draw upon tsunami time-series data for use as boundary conditions for the inundation modelling. The selection of information from the databases for modelling purposes is described in Section 3.5.3.

The tsunami databases are a key input to the study as their data drive the hydrodynamic inundation model (Section 5) to allow for broad scale ocean information to be translated into how tsunami behave when they reach land (i.e. determine the extent of coastal inundation).

3.5.1 Tsu-DAT (Geoscience Australia)

Tsu-DAT provides a tool to access GA's database of numerical modelling results of thousands of individual synthetic tsunami events and provides a summary, in terms of both probability and average recurrence interval (ARI), of the likelihood of a given tsunami height occurring at a given offshore location (at the 100m depth contour). Furthermore, it allows the interrogation of which tsunamigenic sources that a particular magnitude tsunami may originate from. Tsu-DAT was provided, under license agreement, to Cardno by the NSW SES for the purposes of this study. The general intention of the tool is to inform emergency management planning and is not intended for real time emergency management purposes.

Data within the Tsu-DAT tool was derived from the *Probabilistic Tsunami Hazard Assessment (PTHA) of Australia* (Burbidge et al, 2008). This assessment modelled thousands (76,000+ in total) of synthetic tsunami to estimate the likelihood of a tsunami wave of a given amplitude occurring at an offshore location, defined at the 100 m depth contour (Geoscience Australia, 2010b). Tsunami generated from sources other than subduction zones were not included in the hazard assessment. The focus on subduction zones in the southeast Indian and Pacific Oceans is justified because these are known to have produced major historical tsunami and are considered the most likely source of future events (BoM, 2010).

The general approach taken within the PTHA can be summarised as follows (Burbidge, 2010):-

- Create a fault model and define possible earthquake events along these fault lines;
- Model the tsunami from each sub-fault event to the coast;
- Sum the sub-fault tsunami together for each earthquake;
- Calculate the probability for each earthquake;
- Calculate maximum wave height at a given probability or probability of exceeding a given height.

Due to its probabilistic nature, Tsu-DAT was able to provide this study with offshore tsunami heights for a range of recurrence intervals at the individual study sites. It also allowed the identification of which subduction zones pose a particular hazard at a given recurrence interval. To this end, the Tsu-DAT tool was used to define which tsunami scenarios would be simulated as part of the inundation modelling task. Further description of the selection process is provided in Section 4.

3.5.2 T2 Database (Bureau of Meteorology)

The BoM's T2 database includes output from the numerical modelling of thousands of hypothetical tsunami events, in terms of water level and depth-averaged velocity signals. The T2 database has been developed to inform the *Australian Tsunami Warning System* with the aim of providing numerical predictions of tsunami events based on observed earthquake magnitudes, seismic moments and location. It is intended to be used as a predictive tool within real time emergency management systems.

The T2 database contains tsunami wave signals that are the results from a prescribed set of modelled events given in Table 3.1. These tsunami signals are generated by earthquakes of magnitudes (M_w) of 7.5, 8.0, 8.5, and 9.0 from all subduction zones within the Indian and Pacific Oceans (Figure 2.2). This series of pre-

computed scenarios form the basis of the Joint Australian Tsunami Warning Centre's real-time tsunami warning system.

Table 3-1: T2 Scenario Database Assumed Initial Condition Details (from Greenslade et. al., 2009)

Magnitude (M_w)	Rupture Width (km)	Number of Rupture Elements	Rupture Length (approx.) (km)	Slip – u_o (m)
7.5	50	1	100	1
8	65	2	200	2.2
8.5	80	4	400	5
9	100	10	1000	8.8

Each subduction zone is split into a series of rupture elements at 100km spacings and as such each rupture event is made up of one or more rupture elements depending on the magnitude and rupture length of the event being simulated. A series of magnitude M_w 8 events, for example, are then investigated for each subduction zone by shifting the centroid along by one rupture element at a time. In this way, tsunami for a range of magnitude ruptures are available at any location along a subduction zone.

For tsunami that are generated by earthquakes with magnitudes in between the prescribed event values shown in Table 3.1, tsunami signals can be generated by using the same rupture length and width as the nearest prescribed event, but with a slip (and thus a wave height / water level time-series) that is modified by a scaling factor, F_S. This scaling factor can be determined from the equation shown below (Greenslade et. al., 2009):-

$$F_S = 10^{\frac{3}{2}\left(M_{W(INT)} - M_W\right)}$$

Thus to obtain tsunami wave time-series signals for intermediate magnitudes ($M_{w(INT)}$), the process is simply to extract the signal resulting from an earthquake of the nearest magnitude (shown in bold in Table 3.2) and then multiply the resulting signal by the scaling factor F_S. Table 3.2 summarises the outcomes of this scaling process.

Table 3-2: T2 Scenario Database Assumed Initial Condition Details (from Greenslade et. al., 2009)

Event Magnitude (M_w)	Nearest Magnitude (M_w)	Scaling Factor (F_s)	Slip - $F_s u_o$ (m)	Rupture Width (km)	Rupture Length (km)
7.3	7.5	0.5	0.5	50	100
7.4	7.5	0.71	0.71	50	100
7.5	7.5	1	1	50	100
7.6	7.5	1.41	1.41	50	100
7.7	7.5	1.9	1.9	50	100
7.8	8	0.52	1.14	65	200
7.9	8	0.71	1.56	65	200
8	8	1	2.2	65	200

Event Magnitude (M_w)	Nearest Magnitude (M_w)	Scaling Factor (F_s)	Slip - $F_s u_o$ (m)	Rupture Width (km)	Rupture Length (km)
8.1	8	1.41	3.1	65	200
8.2	8	1.9	4.18	65	200
8.3	8.5	0.52	2.6	80	400
8.4	8.5	0.71	3.55	80	400
8.5	8.5	1	5	80	400
8.6	8.5	1.41	7.05	80	400
8.7	8.5	1.9	9.5	80	400
8.8	9	0.53	4.66	100	1000
8.9	9	0.71	6.25	100	1000
9	9	1	8.8	100	1000
9.1	9	1.41	12.41	100	1000
9.2	9	2	17.6	100	1000

Output from the T2 database includes full time series information at any grid point in the propagation model domain. This has particular advantages for the application of boundary conditions to the inundation modelling (Section 6). As such, scenarios from the T2 database were used for this purpose.

3.5.3 Database Utilisation for this Assessment

After discussions with the Steering Committee (Section 1.4) regarding the selection of tsunami events, a collaborative approach was agreed upon, which made use of information from both databases. It was agreed that initial identification of the tsunami risk and individual events would be made using GA's Tsunami Data Access Tool (Tsu-DAT) and subsequent tsunami time-series for use as boundary conditions for the inundation modelling would be taken from the BoM's Enhanced Tsunami Scenario Database: T2 (T2 database).

One primary difference between the two databases is how the initial ruptures that generate tsunami are modelled. Tsu-DAT dissects each subduction zone into a series of sub-faults and each rupture event (which is made up of one or more adjacent sub-faults) has been described through detailed analysis of probable earthquakes and associated ruptures. There is no prescriptive formulation describing the number and form of rupture elements.

The T2 database also discretises each subduction zone into rupture elements; however, a simulated rupture event (scenario) is made up of a prescribed number of rupture elements, each with a defined rupture length and width based on its moment magnitude (M_w), so that an M_w8 event consists of two rupture elements and an M_w9, ten rupture elements (see Table 3.1).

Each database has particular advantages to this project and hence an approach incorporating both sets of information has been developed. Tsu-DAT is a useful tool for identifying from where tsunami events, which pose a risk to a given site, may originate and how often these may occur in a probability risk based approach. The T2 database provides tsunami time-series at any location/contour depth within the BoM's model domain

allowing the extraction of boundary information for each inundation model to be from seaward of the continental shelf edge before significant shoaling has occurred. This is preferable for inundation modelling to ensure that the correct hydrodynamics of the shallow water tsunami wave are being generated within the Delft3D inundation model (Section 6). It also allows for a verification of the Delft3D inundation model using time-series data from locations inshore from the adopted inundation model boundaries, also extracted from the BoM T2 Database, for both water levels and currents.

4 TSUNAMI SCENARIOS

Emergency response planning (which this study seeks to inform) is required to consider the full range of possible tsunami magnitudes. That is, from lower magnitude tsunami impacting the marine and immediate foreshore environment, through the range of tsunami events of increasing magnitudes resulting in land inundation threat and including the worst case or 'highest credible threat' event.

Tsunami magnitudes up to the 10,000 year ARI event were considered for this study, this being of a similar order to concepts such as the Probable Maximum Flood (PMF) in flood/coastal engineering terminology. However, it is important to note that data are available for magnitudes up to the 100,000 year ARI and therefore there is still potential for the inundation information prepared for this assessment to be exceeded.

This study does not seek to establish specific emergency response planning thresholds but serves to inform the discussion of any requirement for consideration of tsunami in an emergency management and land use planning context. To this end, it is necessary to investigate a range of tsunami magnitudes that are related to risk levels in terms of likely occurrence. This process is described below.

4.1 Event Selection Approach

Using the available information within Tsu-DAT (Section 3.5.1), a methodology was developed to identify the most appropriate tsunamigenic sources and events to simulate. This methodology is summarised in the flow chart below.

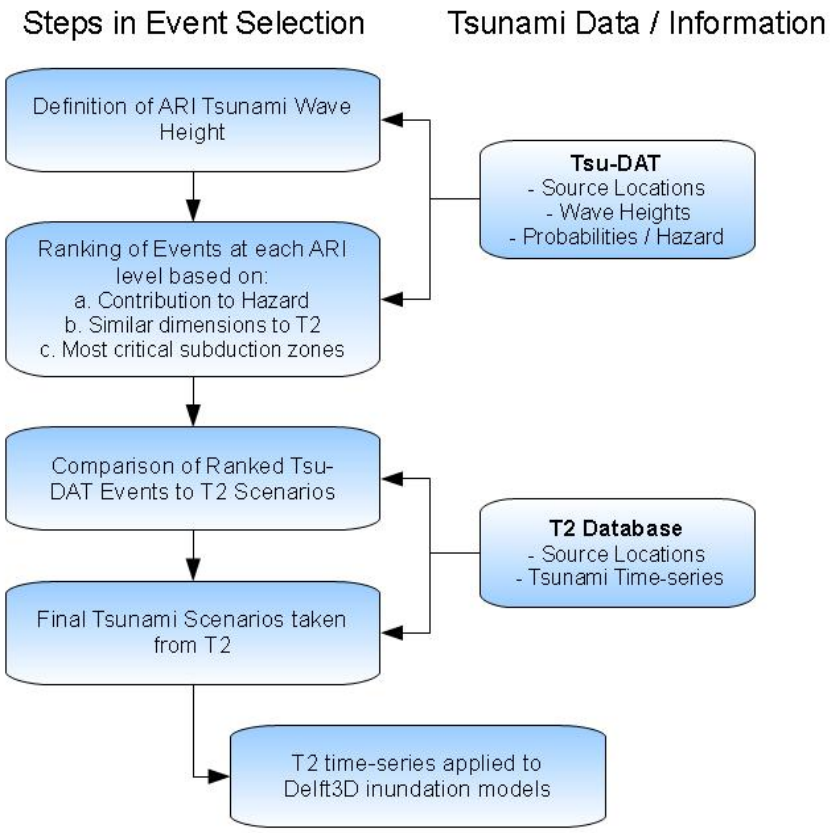

From Tsu-DAT it was found that a number of subduction zones (Figure 2.2) contribute to the risk of encountering a higher probability (100 to 500-years ARI, for example) event, in terms of wave height, at the 100m depth contour along the NSW coast. At lower probability levels (10,000-years ARI, for example), events may potentially occur from fewer subduction zones.

Table 4.1 summarises the range of tsunami events selected for simulation at each site using the numerical models. As outlined above, the number of events from different subduction zones (ranging between 2 and 5) is representative of the number of potential sources, identified by Tsu-DAT, for each average recurrence interval (ARI).

Table 4-1: Summary of Tsunami Events Simulated for each Site

ARI (years)	Number of Tsunami Sources (Subduction Zones)		Total Number of Modelled Events
	HAT Tide Level	MSL Tide Level	
200	5	-	5
500	4	-	4
1000	3	-	3
2000	3	3	6
5000	2	2	4
10000	2	-	2
Total Modelled Events per Site			24

Table 4.1 indicates that the simulations generally focus on the worst case scenario; that is, a tsunami occurring at high water (HAT). It should be noted that while this seems conservative, non-astronomic contributors to coastal water levels (such as meteorological effects) results in these levels being reached or exceeded several times a year. However, the 2000 and 5000-years ARI magnitudes have also been investigated for a mean sea level scenario (MSL, not including any allowances for climate change induced sea level rise). This combination of tide investigations is based on previous studies where a significant inundation threshold was observed at around a 2000 year ARI event (pers. comm. David Hanslow and Simon Opper). The adoption of two tide levels for two of the ARI's provides for some investigation of sensitivity to tidal level/phase, noting that tsunami waves persist for some hours and would most likely encounter a high tide, even if not at a time of the highest tsunami waves.

In interpreting the information in Table 4.1 it is important to note that:

- A tsunami of a particular ARI at an epicentre does not necessarily become the equivalent ARI tsunami (in terms of wave height / wave run-up) at any inshore location. Therefore, tsunami magnitudes have been defined locally (i.e. at the 100m depth contour) at each of the study sites.

- Tsunami run-up and inundation at a particular point will be influenced by a range of factors including nearshore features, position/exposure of a location within an embayment and general alignment to the tsunami wave. That is, tsunami inundation will be significantly influenced by the orientation of the coastline and the interaction of the nearshore region and the incoming tsunami, in terms of both direction and periods of the individual waves. Hence it is considered prudent to assess a range of tsunamigenic sources (hence the selection of 2 – 5 sources for any given ARI).

4.2 Event Selection from Tsu-DAT

Tsu-DAT summarises a range of data useful to the selection of tsunami events. At the 100m depth contour (the selected input point for the inundation modelling) it provides the wave height for a range of tsunami recurrence intervals. Using this data it is therefore possible to identify all events that generate a wave height within each ARI as a 'confidence band' (i.e. a value plus or minus a value). For example, for the 500 year ARI event the wave height is 0.57m +/-0.05m at the 100 m depth contour offshore of Botany Bay. By using the confidence band approach this reduces the number of relevant events in the database by two orders of magnitude. For example, for the 500 year ARI this reduces the number of relevant events from 76,000+ (total in the database) to approximately 500 at each of the study sites.

Tsu-DAT also presents the influence of each sub-fault within a subduction zone to the selected recurrence level, through the percentage contribution to hazard. This measure refers to the contribution of a given rupture element in producing the tsunami wave height at given location and recurrence interval. Figure 4.1 provides an example of this for the 500 year ARI (for a particular inshore location) along the New Hebrides subduction zone (Figure 2.2). A single rupture event, which generates a tsunami, may consist of a number of adjacent sub-faults. Knowing which sub-faults make up each of these rupture events, it is possible to rank each rupture event according to its average percentage contribution to hazard per subfault.

Ranking events based on the average of the percentage contribution to hazard does not necessarily identify specific events most likely to occur (that is, with the highest probability), but rather it ranks events based on their location along the fault line. Higher weighting is therefore given to events that occur along parts of the subduction zone from which tsunami are most likely to occur. Considering the average and not the cumulative contribution to hazard ensures that the ranking is not skewed to the larger (in terms of length and number of sub-faults) rupture events. This analysis therefore provided an efficient way of identifying the most appropriate rupture events to consider from approximately 500 events that contribute to the 500 year ARI confidence band.

Boundary conditions for inundation modelling were ultimately obtained from the T2 database (Section 3.5.2 and Section 4.3) so it was also necessary to find events within the Tsu-DAT database that fit the prescribed T2 scenario dimensions, in terms of rupture size. That is, scenarios are defined within the T2 database using standard initial conditions for various earthquake magnitudes (Section 3.5.2). This was done to ensure that boundary conditions from the T2 database (Section 4.3) will be as close as possible a match to the selected outcomes of Tsu-DAT.

The identification of appropriate events from Tsu-DAT was therefore undertaken on the following basis:-

1. Ranking of events from all subduction zones with the largest average contribution to hazard.
2. Selection of events from all subduction zones with similar dimensions to the T2 database (in terms of moment magnitude, rupture length and slip).
3. Identification of the most critical source zones within the full range of subduction zones based on the above two criterion (to account for tsunami direction/wave period variability).

Preference was also given to those events with wave heights at the upper end of the ARI confidence band provided by Tsu-DAT.

The same set of critical source zones (subduction zones) were selected for each study site (Section 1.2) based on the information within Tsu-DAT. These are summarised in Table 4.2 (and the locations are shown in Figure 2.2).

Table 4-2: Critical Source Zones (Subduction Zones) for Study Sites

ARI (years)	Subduction Zone				
	Puysegur	New Hebrides	Kermadec	Tonga	South Chile
200	X	X	X	X	X
500	X	X	X	X	-
1000	X	X	X	-	-
2000	X	X	X	-	-
5000	X	X	-	-	-
10000	X	X	-	-	-

The subduction zones (Table 4.2) identified through the process outlined above represent zones which generate tsunami of a range of approaching directions and alignments to the individual NSW coastal study sites (Section 1.2). This ensures that any localised sensitivities at the study sites are included in the investigation.

However, while the set of critical source zones (subduction zones) are the same, the individual events simulated from these zones are unique for each study site (see Section 4.3).

4.3 Boundary Conditions for Inundation Modelling

Interrogation of the Tsu-DAT database using the methodology outlined in Section 4.2 resulted in the identification of the most appropriate events (from each of the contributing subduction zones) for inundation modelling; given the fact that the boundary conditions to the Delft3D inundation model (Section 6) were to be extracted from the BoM's T2 Database. Thus, in order to gain consistency in the tsunami selection process it was necessary to reconcile the two different databases.

Comparison of tsunami modelling systems and/or approaches is notoriously troublesome. Differences in the description of the rupture events, bathymetric datasets, resolution of the numerical grid and the propagation schemes typically result in vastly different tsunami signals at a given location. This is particularly the case for nearshore tsunami amplitudes which are strongly dependent on the water depth (Greenslade et. al., 2010). In fact, the models that underpin the data in the T2 (BoM) and Tsu-DAT (GA) databases use different bathymetric datasets and therefore the geographic location of the 100m contour is not the same, as shown in Figure 4.2. Figure 4.2 shows a contour from the T2 database (produced from the T2 bathymetric dataset) and hazard points for the Tsu-DAT database (locations of available output from Tsu-DAT at the 100m depth). Furthermore, at the 100m depth contour the resolution of the models used to generate the data in the databases is 1km in the Tsu-DAT source model and between 6 and 7.5km in the T2 source model.

It was therefore considered more appropriate to compare tsunami wave heights from the 100m depth from the two databases rather than at the same coordinate location. In this way, the extracted tsunami signals would have undergone a similar amount of shoaling and directional change. Tsunami signals from the T2 database were extracted along the 100m depth contour at locations as close as possible to the relevant Tsu-DAT hazard points (Figure 4.2) for each of the critical subduction zones defined in Table 4.2.

As outlined in Section 3.5.2, the T2 database only incorporates the results of the analysis of specific earthquake magnitudes. For scenarios between the modelled magnitudes in the T2 database, termed 'intermediate scenarios', scaling of the wave height (via the time-series output) was undertaken from the nearest prescribed magnitude, as described in Table 3.2. The range of possible T2 wave heights (for M_w7.3 to 9.2) were then extracted and scaled for each of the selected subduction zones (Table 4.2). An example of the resulting distribution of T2 wave heights using this process for the wave height offshore of Merimbula, from the Tonga subduction zone (T2 rupture element 246) is presented in Figure 4.3.

This wave height distribution was then used to find a Tsu-DAT event (from the list of appropriate events) that matched an available T2 event in terms of both moment magnitude (M_w) and wave height for each recurrence level (ARI) and subduction zone. A difference in wave heights of less than 10% was sought.

As outlined in Section 4.1, 19 tsunami events were identified from the T2 database for each site, five of which were run at two tide levels (as shown in Table 4.1). The selected T2 events along with the corresponding Tsu-DAT event are summarised in Appendix A.

This matching process allowed for very close matches between wave heights from Tsu-DAT and T2 at lower ARI levels, however, for ARI's upward of 2000-years, finding a close match proved difficult. This is due to the logarithmic nature of the resultant wave heights as M_w increases within T2 (Figure 4.3). In some instances, the difference in wave height between higher ARI events was found to be quite large, resulting in T2 either underestimating or overestimating the Tsu-DAT wave height significantly.

In some circumstances T2 was unable to provide wave heights of sufficient magnitude to match Tsu-DAT at a given recurrence interval (noting that scaling is limited to M_w9.2 within T2). However, when the scaling formula (Section 3.5.2) was used to scale up to M_w9.3, reasonable matches could be found with Tsu-DAT events. It is therefore considered, that for this task scaling to M_w9.3 is justified as the resulting wave heights are verified against the outcomes presented in Tsu-DAT. Subsequent advice from the BoM has confirmed

that reasonable scaling beyond M_w9.2 is realistic and compares well to the rupture dimensions of recent events (pers. comm. D. Greenslade).

At the end of this matching process, the input boundary conditions (prescribed as water level signals for the various recurrence intervals) were ready for use in the inundation modelling (Section 6.5).

It should be noted that in some cases, the range of magnitudes (M_w) for a T2 scenario did not provide adequate resolution to distinguish between 2 events of different ARI's. An example of this can be found in Appendix A – Table A.1, where for Swansea a 1000yr event from New Hebrides has a Tsu-DAT wave height of 0.871m and a 2000yr event from New Hebrides has a Tsu-DAT wave height of 1.02m. The closest T2 scenario to both of these events is 194d, which gives a 0.94m wave height.

In such a case, where the selection process converges on a single T2 scenario for two sequential recurrence interval cases, linear interpolation was applied to the T2 signal, to scale it up or down to the recommended Tsu-DAT wave heights at each recurrence interval. The validity of this approach was first tested to ensure that a tsunami scaled by a certain factor (n) on the boundary, resulted in tsunami waves that were scaled by the same factor (n) at inshore locations.

To this end a series of models were run, the first using an unscaled T2 scenario as boundary conditions, and a second run using a scaled T2 scenario, in this case a factor of 0.8. The results are presented in Figure 4.4 for T2 Scenario 310d (from Honshu, Japan). Comparisons of the two inshore tsunami signals show that the maximum wave height scales linearly at inshore locations, and that general characteristics, such as wave period, of the signal remain unchanged.

Therefore linear scaling is valid for situations where more than one event is represented by the same T2 scenario and was utilised in the scenario modelling.

5 MODEL SYSTEM

The Delft3D hydrodynamic modelling system was applied for this study (Deltares, 2010 – FLOW version 3.28.10). This hydrodynamic modelling system is a world leading hydrodynamic model which has been extensively utilised at sites around Australia and internationally. The Delft3D system has been demonstrated to be very accurate when used for tsunami modelling undertaken for the UNHCR following the 2004 Boxing Day tsunami (Wilkinson, 2005)

The following section provides a brief introduction to the numerical scheme and application of the Delft3D model system.

5.1 Delft3D FLOW

Investigations of water levels, currents, transport-dispersion and turbulent processes require the application of a high level model capable of simulating a range of processes including: ocean wave and tidal forcing, with some confidence. Such simulations can be successfully undertaken using the Delft3D modelling system.

This modelling system can include wind, pressure, tide and wave forcing, three-dimensional currents, stratification, sediment transport and water quality descriptions and is capable of using irregular rectilinear or curvilinear coordinates.

Delft3D is comprised of several modules that provide the facility to undertake a range of studies. All studies generally begin with the hydrodynamic Delft3D-FLOW module. From Delft3D-FLOW, details such as velocities, water levels, density, salinity, vertical eddy viscosity and vertical eddy diffusivity can be provided as inputs to the other modules. The wave and sediment transport modules work interactively with the FLOW module through a common communications file.

5.1.1 Hydrodynamic Numerical Scheme

The Delft3D-FLOW module is based on the robust numerical finite-difference scheme developed by Stelling (1984) at the Delft Technical University in The Netherlands. Since its inception the Stelling Scheme has undergone considerable development and review by Stelling and others.

The Delft3D Stelling Scheme arranges modelled variables on a horizontal staggered finite difference Arakawa C-grid. The water level points (pressure points) are designated in the centre of a continuity cell and the velocity components are perpendicular to the grid cell faces. Finite difference staggered grids have several advantages including: -

- Boundary conditions can be implemented in the scheme easily;
- It is possible to use a smaller number of discrete state variables in comparison with discretisations on non-staggered grids to obtain the same accuracy;
- Staggered grids minimise spatial oscillations in the water levels.

Delft3D can be operated in two-dimensional (2D) (vertically averaged) or three-dimensional (3D) mode. For

this project the model was operated in 2D, this being appropriate for the simulation of shallow water waves and inundation modelling. This also ensured that the model was computationally efficient.

Delft3D allows the application of a specialised advection scheme that can be implemented for problems that include rapidly varying flows for instance in hydraulic jumps, bores and tsunami inundation (Stelling and Duinmeijer, 2003). The scheme is denoted as the 'Flooding Scheme' and was developed for 2D simulations with a rectilinear grid for the inundation of dry land with obstacles such as road embankments and levees. The integration of the advection term is explicit and the time step is restricted by the Courant number for advection.

The model is particularly robust when applied to rapidly varying depth-averaged flows, for instance, the inundation of dry land or flow transitions due to large gradients of the bathymetry (obstacles). The scheme is also accurate for obstacles, represented by only one point on coarse grids. In combination with the local invalidity of the hydrostatic pressure assumption, conservation properties become crucial. In flow expansions a numerical approximation is applied that is consistent with conservation of momentum and in flow contractions a numerical approximation is applied that is consistent with the Bernoulli equation.

Horizontal solution is undertaken using the Alternating Direction Implicit (ADI) method of Leendertse for shallow water equations. Vertical turbulence closure in Delft3D is based on the eddy viscosity concept.

5.1.2 Wetting and Drying Algorithm

Many nearshore areas include shallow inter-tidal regions; consequently Delft3D includes a robust and efficient wetting and drying algorithm to handle this process. In combination with the flooding scheme for advection in the momentum equation, the algorithm is also effective and accurate for rapidly varying flows with large water level gradients because of the presence of hydraulic jumps or the occurrence of bores as a result of dam breaks. This capability ensures the applicability of Delft3D to tsunami inundation modelling.

5.1.3 Conservation of Mass

Problems with conservation of mass found in some numerical models, such as a 'leaking mesh', do not occur within the Delft3D system. However, whilst the Delft3D scheme is unconditionally stable, inexperienced use of Delft3D, as with most modelling packages, can result in potential mass imbalances.

Potential causes of mass imbalance and other inaccuracies include: -

- Inappropriately large setting of the wet/dry algorithm and unrefined inter-tidal grid definition
- Inappropriate bathymetric and boundary definition causing steep gradients
- Inappropriate time step selection (i.e. lack of observation of the scheme's allowable courant number condition) for simulation.

The DELFT3D model has been schematised for the tsunami inundation modelling to ensure that these potential causes of mass imbalance have been avoided.

5.1.4 Domain Decomposition

Delft3D provides the facility to adopt a modelling approach known as 'domain decomposition'. Domain decomposition is a technique in which a model is divided into several smaller model domains that are dynamically coupled. The subdivision is based on the horizontal and vertical model resolution required for adequately simulating physical processes. Computations can be carried out separately, yet concurrently, on these domains. The communication between the domains takes place along internal boundaries. Computations are carried out concurrently, via parallel computing, thus reducing the turn-around time of multiple domain simulations. Domain decomposition allows for local grid refinement, both in the horizontal direction and in the vertical direction in 3D models. Grid refinement in the horizontal direction means that in one domain smaller mesh sizes (fine grid) are used than in other domains (coarse grid). In the case of vertical grid refinement one domain, for example, uses ten vertical layers and another domain five layers, or a single layer (depth-averaged).

Domain decomposition is widely recognised as an efficient and flexible tool for the simulation of complex physical processes. The structured multi-domain approach combines the advantages of the modelling flexibility of the single-domain unstructured approach with the efficiency and accuracy of the single-domain structured approach.

5.2 Model System Validation and Verification

Following the Indian Ocean tsunami of Boxing Day (26 December) 2004, there has been substantial interest in developing tsunami mitigation plans for tsunami-prone regions worldwide (Synolakis et al, 2008). In response to this, the United Nations Educational, Scientific and Cultural Organisation (UNESCO) has been attempting to establish intergovernmental coordination mechanisms for tsunami hazard mapping to inform the preparation of such mitigation plans. The need for such plans and mapping has become even more evident in the wake of the devastating Pacific tsunami on 11 March 2011.

Due to the fact that there are a large number of different organisational bodies in the Pacific, Atlantic and Indian Ocean regions, there is some risk that tsunami forecast products may be produced with outdated or even unproven methodologies. This is a global hindrance, as the Intergovernmental Oceanographic Commission (IOC) of UNESCO discovered in its attempts to assist its member nations in developing tsunami hazard maps (Synolakis et al, 2008). Unrealistic estimates can be costly. Estimates that under predict a tsunami threat can put lives at risk, whereas estimates that over predict can result unnecessary evacuations and lead to panic, reducing the credibility of the world system. To this end, certain standards (for example, NOAA (2007) and a range of working papers compiled by the various Intergovernmental Coordination Groups working under UNESCO/IOC – see http://www.ioc-tsunami.org/) have been implemented to ensure a minimum level of quality and reliability for real-time forecasting and inundation mapping products.

In order to calculate tsunami currents, forces, and inundation extents of coastlines it is necessary to calculate the progression of the tsunami waves from the deep ocean into the coast. Regardless of the type of numerical model, both validation (the process of ensuring that the model solves the parent equations of motion accurately) and verification (the process of ensuring that the model represents geophysical reality appropriately) are an essential part of the model development.

5.2.1 Model Validation

Many existing numerical models (such as Delft3D) have been validated with comparisons to numerical solutions. Details of the numerical validation of Delft3D can be found in Deltares (2010).

5.2.2 Model Verification

Site specific data of a tsunami of a sufficient magnitude to show a reasonable amount of inundation for the New South Wales coastline to undertake direct numerical model verification was not available for this study. As such, the Delft3D model setups at the five NSW sites (Section 1.2) could not be directly verified. A description of the indirect calibration and validation process for the study sites is provided in Section 7.

To overcome the lack of site-specific field data, the National Oceanic and Atmospheric Administration (NOAA) in the USA have recommended a series of 'benchmark' events to be replicated in order to validate models (NOAA, 2007). This is referred to as 'benchmark verification' and this process provides confidence in the model system utilised where site specific data do not exist.

Data from the 1993 Okushiri Island (northern Japan) tsunami event was used as the 'benchmark verification' case for the Delft3D model used for this assessment.

Event Overview and Field Data

On 12 July 1993, a magnitude M_w7.8 earthquake occurred with the epicentre located at 42.76^{O}N and 139.32^{O}E, off the south western coast of Hokkaido, Japan near Okushiri Island (see Figure 5.1). The coastline of both Okushiri Island and the Oshima Peninsula of Hokkaido were affected by the event. Field data (e.g. run-up height and water levels at gauges) were available for the model validation for the event at locations including at Monai and Aonae (Okushiri Island) and Iwanai and Esashi (on the Oshima Peninsula of Hokkaido).

Field surveys by a number of authorities and institutions following the event were undertaken that provided a spatial description of tsunami run-up around Okushiri Island (Takahashi, 1994). Unusual features of the observed tsunami, included:

- An extreme run-up height of 31.7 mMSL measured near the village of Monai. This tsunami run-up mark was discovered at the tip of a very narrow gulley within a small cove (CRIEPI, 2004). It is considered that the large run-up height was a result of unique and complex bathymetric and topographic features.
- The arrival of the first wave at a location known as Aonae, five minutes after the earthquake and a second wave, 10 minutes after the first. The first wave came from the west, while the second wave came from the east.

Physical Modelling

In addition to the field surveys, a 1:400 scale laboratory experiment of the Monai Valley for the tsunami event was established, using a physical model tank at the Central Research Institute for Electric Power Industry (CRIEPI) in Abiko, Japan. The primary objective for the physical model was to replicate the water level signal

at three output locations (referred to as Channel 5, 7 and 9) as well as the maximum run-up level. This data provides a point of reference for numerical simulations.

Delft3D Modelling

To conduct the benchmark verification, a Delft3D model system was created for the Okushiri Island area using the same model parameters as that adopted for the five NSW Tsunami Inundation Models. The Disaster Control Research Centre (DCRC), Japan, digitised the bathymetric and topographic data from several sources and this publicly available data (Matsuyama and Tanaka, 2001) was used in the development of the Delft3D model grid.

DCRC also constructed an initial wave profile from a 1.1m subsidence (depression) and two separate water level uplifts along the subduction zone of 4.9m and 2.2m respectively. This initial water level variance can be seen in Figure 5.2 and this was used for the model initial conditions.

Figures 5.3 and 5.4 show key outcomes of the Delft3D simulation at Monai in terms of modelled versus observed run-up and modelled versus observed physical model water level information. The extreme wave run-up near Monai village is replicated by the Delft3D model, with a level of 32mMSL being achieved (compared to 31.7mMSL recorded). Furthermore, a comparison of the time series water level data at the three physical model wave gauge locations show that the Delft3D model reproduces both the tsunami signal peaks and phasing extremely well. Some discrepancy between the signals may result from the initial condition in the physical model, which is different from the numerical model description at time zero in the simulation. The cause of this initial difference is unknown although has been observed during other model validation tasks (Nielson et. al., 2005).

Model output as water levels for two snapshots in time at Aonae is presented in Figure 5.5. This shows that the initial wave comes from the west and arrives five minutes after the earthquake event, and this is followed approximately 10 minutes later by a second wave coming from the east as per the observed conditions.

The Delft3D results also provide a reasonable match to the tide gauge data at Iwanai and Esashi, as shown in Figure 5.6, particularly given the uncertainties in the initial sea surface uplift. Furthermore, the exact location of the tide gauges was not available and it was therefore not possible to achieve a better match. Tsunami wave height and phasing signals can vary significantly over relatively small distances and thus without knowing the exact location of the tidal gauges providing a more detailed comparison is difficult, and only a reasonable estimate can be offered.

Figure 5.7 shows that the run-up levels around Okushiri Island closely resemble those of the measured/observed data. The spatial variability of run-up levels around the island are reproduced very well, with all major variations described. Furthermore the run-up in the small valley to the north of Monai reaches 32.0m, a close match to the 31.7m measured after the event.

As a result of the close agreement between the Delft3D model results and the Okushiri benchmark data, the Delft3D modelling system has demonstrated a reasonable level of accuracy and can be considered verified. As such, its use in the NSW Tsunami Inundation study is considered appropriate.

6 DESCRIPTION OF INUNDATION MODELS

Inundation models covering each of the study sites (Section 1.2) were established using the Delft3D software. As described in Section 5.2, the Delft3D numerical scheme has been adopted in many tsunami studies worldwide and has been compared to world standard benchmark verifications with good agreement.

6.1 Overview

Modelling of tsunami inundation can be undertaken in a number of ways. The typical approaches include:-

- Modelling of tsunami from the tsunamigenic source; and
- Modelling of tsunami starting from a selected inshore contour through a nested model setup (using external source data to translate the tsunami from source to the inshore contour).

This study has adopted the latter approach due to the availability of well established tsunami databases, which include detailed analyses of potential tsunami sources that affect the NSW coastline. These databases, namely Tsu-DAT (from GA) and T2 (from the BoM), were provided for use in event selection and the preparation of boundary conditions for the inundation modelling (Section 3.5).

6.2 Description of Typical Model Setup

The extent and size of the individual study area grids (for bathymetry/topography and roughness) vary depending on site specific features such as landforms (headlands and embayments) and the topographic lie of the land. The model extents were discussed with the Steering Committee (Section 1.4) before their finalisation for use in this assessment. The data to define the bathymetry and topography used in the model set up is outlined in Section 3.1.

Regional models were constructed for each site and utilised the 'domain decomposition' structured grid system in Delft3D (Section 5.1.4). Model systems at each site typically consisted of three to five grids and extended approximately 50km north and south of each specific study area and out beyond the 3000m depth contour (between 50 and 100km offshore). This practice ensured that issues associated with high frequency boundary reflections were avoided at the offshore boundary. On land the grid extends up to the 15mAHD contour which covers the possible extent of coastal inundation at these sites.

The grid resolution for the overland sections of the model is in the order of 10m. The appropriateness of this grid resolution is further discussed in Section 7.5.2 and is considered to adequately describe the overland terrain for the purposes of inundation modelling and hazard extent definition. The offshore resolution is 500m with increasing grid resolution for each nested grid.

The grid layouts developed for each study site are presented in Figures 6.1 to 6.5.

6.3 Overland Flow Schematisation

The five study sites (Section 1.2) chosen for this investigation include large areas of commercial and

residential development. Typically, overland flow studies have taken account of such areas by either specifying individual structures (e.g. building footprints) or applying an increased roughness parameter to account for such features. The designation of individual structures in the model generally requires a high level of detail and demands a corresponding grid resolution in the order of 1m to 2m; compared with the 10m grids adopted for this study. To overcome this intensive data requirement, characteristic roughness values for these land areas were adopted to describe the attenuation of overland flow through specific areas (residential, commercial, parkland etc.).

6.4 Overview of Computational Approach to Boundary Conditions

Modelling tsunami from inshore depths has a number of advantages over simulating events from the source. It allows for a reduction in model grid coverage and hence the application of greater resolution over the areas of interest without imparting onerous computational times on the inundation simulations. Also, it allows for the use of tsunami databases with an extensive catalogue of tsunami events.

Deflt3D allows the specification of either water level or 'Riemann' boundary conditions (essentially a velocity-based boundary) that are appropriate for simulating tsunami signals. Given that the boundary conditions for the inundation model were being taken from the T2 database (Section 3.5.2, which provides water level and velocities), full use of the available parameters would be desirable in order to correctly describe the tsunami wave, especially in terms of wave direction. This is possible through the use of a 'Riemann' boundary and calculation of 'Riemann Invariants'. However, such a boundary specification requires the grid alignment to be perpendicular (as much as possible) to the incoming waves to minimise the error in the boundary signal. This is caused by the fact that in Delft3D only normal velocities can be prescribed. Such a limitation in setup is not desirable as modelling tsunami from a number of sources, as was done in this study, would require the establishment of an equal number of grid setups.

Therefore, the application of a water level only boundary was considered the most appropriate boundary specification using the model selected for the assessment. In doing so, there exists a potential for shorter period reflections to be generated along boundaries in sufficiently shallow water. This can be overcome in Delft3D by prescribing the boundaries as 'weakly reflective', with the introduction of a damping/reflection parameter. However, such a condition removes some control of the water level being specified at the boundary, and hence rather than using this approach at the offshore boundary it is more appropriate to locate these boundaries in sufficiently deep water where the weakly reflective condition is not required.

6.5 Adopted Boundary Conditions

For the reasons outlined in Section 6.4, the tsunami models were driven by the use of water level time-series along the open boundaries of the model. The offshore boundaries were located beyond the continental shelf in approximately 3000m of water to ensure that no reflections were generated and that the correct hydrodynamics were established as the tsunami propagated into shallow water over the shelf. This was achievable because the T2 database (Section 3.5.2) provides time-series information at every grid point from its own source propagation model.

However, locating model boundaries in shallow water was unavoidable along the lateral (cross-shore)

boundaries of the model. To this end, a weakly reflective boundary condition was established along the lateral boundaries to ensure that reflections were not generated at shallower nearshore locations on these boundaries.

6.5.1 Open Boundaries – Tsunamigenic Signal

The specification of water levels along the open boundaries of the model does not allow for the direct specification of the direction of the tsunami wave. To this end it was hypothesised that the directionality of the tsunami at the boundary could be achieved by use of a variable water level along the boundary. That is, a phase lag between adjacent boundary points would generate the directionality of each tsunami wave. To achieve this, variable water level points were spaced roughly 10km apart (in line with the T2 resolution) along the entire open boundary extent. For each boundary point, a water level time-series was extracted from the T2 scenario database and interpolated for that location from the nearest T2 grid points. Experimental model testing found this to be a valid approach. This approach is similar to applying a segmented wave maker in a physical model, a well proven procedure.

Details and results of this testing can be found in Section 7.2.

6.5.2 Open Boundaries - Tidal Signal

Tide levels were predicted using 10 offshore deep water tidal constants obtained from the Oregon State University global model of ocean tides (Section 3.2). These tidal constants were used to determine a water level time-series for each boundary point location. The tsunami signal was then superimposed on the tidal signal at each of the variable water level boundary points. Phasing of the two signals was also considered to ensure that the highest tsunami wave height occurred at the desired tidal phase (either HAT or MSL, Section 4.1) for each simulation. This phasing was achieved near the coastline of each model rather than at the model boundary; this being a somewhat subjective process.

7 MODEL CALIBRATION, VERIFICATION AND SENSITIVITY

Calibration and verification of numerical modelling techniques provides confidence in the simulated outcomes. These are necessary steps to enable results from the tsunami inundation to be utilised with confidence.

As outlined in Section 5.2, site-specific data of a tsunami of a magnitude sufficient to show a reasonable amount of inundation on the New South Wales coastline to undertake direct numerical model verification was not available for this study. As such, the Delft3D models set up at the five NSW sites (Section 1.2) could not be directly verified for tsunami inundation. However, normal tidal conditions could be calibrated in some cases to measured tidal data and some indicative tsunami verification simulations were undertaken where tsunami signals could be identified.

The following sections provide a description of the tidal and indirect tsunami calibration and verification exercises undertaken for the models, as well as an investigation into the sensitivity of the results to the main model parameters.

7.1 Tidal Calibration

Each regional oceanographic model domain was calibrated to either predicted or measured (where available) tidal signals. This exercise was carried out to ensure that the model systems correctly describe the propagation of long period shallow water waves from deep to shallow water. Tidal water-level time-series at inshore locations were predicted by running the models using offshore deep water tidal constants to drive the regional oceanographic models, extracted from the TPXOv7.2 global tide model (Section 3.2).

Recorded water levels and predicted tides at inshore locations were used to calibrate the models within the estuarine areas of Lake Macquarie and Lake Merimbula. This exercise was undertaken to ensure that the models at these two sites properly described the attenuation of flow through the lake entrance waterways; this aspect not being as critical at Botany Bay, Manly or Wollongong.

The results of the tidal calibration can be observed in Figures 7.1 to 7.7. The modelled results show a good level of agreement between the predicted and measured signals; particularly in terms of phasing.

7.2 Tsunamigenic Verification

7.2.1 T2 Database Verification

In order to confirm reasonable propagation of the T2 tsunami signals to inshore locations, initial verification of the models was conducted by comparison with signals from the T2 database (Section 3.5.2) at inshore locations. Given that the Delft3D model was required to extend to deep water, ensuring the correct description of tsunami propagation over the continental shelf becomes important, particularly when considering shoaling of the tsunami waves. Thus several tests that compared the wave height, velocity and direction of tsunami propagation against the results provided from the T2 database were undertaken. The results, shown in Figures 7.8 to 7.12, present comparisons at two locations for each model system; one offshore and one inshore. The offshore location, near the Delft3D model boundary, is positioned in about

3000m depth (before the tsunami reaches the continental shelf) and the inshore location was typically in a depth of 30m.

The results show that offshore, near the model boundaries, the Delft3D water levels and velocities match extremely well with the T2 data. However, after the tsunami has propagated across the continental shelf and into shallow water, significant wave refraction and shoaling takes place and the Delft3D model diverges from the T2 database records, showing higher tsunami wave heights, and higher frequency oscillations at inshore locations.

It is likely that the principal reason for this outcome lies in the bathymetric descriptions within each model. Both the bathymetric data used and grid resolutions of the models are different, resulting in inconsistent descriptions of the continental shelf slope. The model underlying the T2 database uses a coarser grid system at these depths, with a grid resolution of approximately 7km, while the Delft3D model has a resolution of 500m. As a result the depths and seabed slope at any given location would vary, leading to the refraction and shoaling of the tsunami being described differently. Additionally this difference in grid size means that the Delft3D model, with its higher resolution, is capable of describing higher frequency oscillations which could not be captured by the lower resolution T2 grid.

This is graphically presented in Figures 7.13A and 7.13B, which describe a shore-normal section of the seabed offshore of Botany Bay. Here it can be seen that as the tsunami travels through the relatively deep water (points A through to D), the Delft3D model shows a very close correlation with the T2 signal. However, as the tsunami propagates across the continental shelf and into shallower water (around point E; approximately 250m depth) the Delft3D model begins to diverge from the T2 data.

7.2.2 Alternative Model Software Verification

Verification of the numerical scheme was also tested by comparison to an alternative overland flow model, namely TUFLOW. This exercise was undertaken to gain a measure of the reliability of the Delft3D numerical flooding scheme. The same model setup (using identical grid, bathymetry, roughness and boundary conditions) was established in TUFLOW. The resulting inundation extent closely resembled the inundation extent obtained with Delft3D as presented in Figure 7.14. This agreement between the two models provides another measure of reliability in terms of the overland flow aspect of the Delft3D modelling.

7.3 Historical Tsunami Validation

Comparisons between Delft3D signals and the BoM's T2 model output at similar inshore locations (presented in Section 7.2.1) showed a difference between the two over the continental shelf. In particular, the Delft3D signals showed higher tsunami wave heights and higher frequency oscillations at inshore locations. While this was a difference from the T2 model output, it was not necessarily a difference from what is physically realistic. Hence, it was important to validate the Delft3D model output to measured tsunami signals (from appropriate tide gauges along the NSW coast) for historical tsunami events.

The first stage in this task was to identify appropriate (actual) events to compare with the adopted modelling approach. The subduction zone earthquake events listed in Table 7.1 resulted in observable tsunami signals,

albeit of small magnitude, at sites along the NSW coast. The BoM subsequently provided scenarios from the T2 database to match these events as closely as possible, having compared each to deep water measurements of the actual events. Those comparisons were not provided to Cardno and hence are not reported herein.

Table 7-1: Identified Seismic Events Causing Tsunami along the NSW Coast

Subduction Zone	Locality	Date	Earthquake Magnitude (Mw)	BoM Recommended T2 Scenario
Japan Trench	Honshu, Japan	11/03/2011	9.0	311c scaled up to 9.0
Peru-Chile Trench	Chile, South America	27/02/2010	8.8	408d scaled down to 8.8
Puysegur Trench	New Zealand South Coast	15/07/2009	7.9	218b scaled down to 7.9
Tonga Trench	Gizo, Solomon Islands	02/04/2007	8.1	172b scaled up to 8.1
Peru-Chile Trench	South Central Chile	22/05/1960	9.5	401d scaled up to 9.2

Note that the BoM did not undertake event specific simulations, but rather they investigated their extensive database of tsunami simulations and identified specific tsunami scenarios that were probably similar in terms of location and magnitude. In this validation exercise it was necessary to scale the available tsunami events and to note that scaling from 8.5Mw to 9Mw does not provide the same time-series of tsunami heights as a 9Mw simulation due to differences in the initial rupture dimensions.

7.3.1 Available Historical Records

A commonly available source of tsunami measurements is tide gauge data, being continuous permanent installations. However, to adequately distinguish a tsunami signal from tidal data the averaging and sampling procedures adopted for the tidal measurements need to be of a sufficient temporal resolution. Typically, tidal measurements along the NSW coast are averaged and recorded over/at 15 minute intervals. This is considered unsuited to accurately characterise a tsunami signal. However, higher frequency gauge data (1 minute averaging and sampling rate) was available at a number of sites along the NSW coast that were appropriate to the sites adopted for this study, namely:-

- Eden Tide Gauge (operated by MHL)
- Port Kembla (operated by Port Kembla Port Corporation, PKPC)
- Botany Bay (operated by Sydney Ports Corporation, SPC)
- Fort Denison (operated by SPC)

These tide gauge locations coincide with 4 of the 5 study sites. While tide gauge data is collected in the Lake Macquarie area, sampling/averaging times are 15minutes, and thus were not appropriate for accurate tsunami identification. Tide gauge data was available at Port Kembla from two separate locations; at the PKPC tide gauge within the inner harbour and at the National Tide Centre (BoM) tide gauge, located in the outer harbour. The availability of tide gauge data is shown below in Table 7.2. Locations of the tide gauges are presented in Figures 6.1 to 6.4.

Table 7-2: Available Quality Assured Tide Gauge Data

Tsunami Event	Sydney Harbour Fort Denison	Botany Bay	Port Kembla Inner Harbour	Port Kembla Outer Harbour	Eden
Honshu, Japan - 11/03/2011	x	x	x	x	x
Chile, South America - 27/02/2010	x	x	-	-	-
New Zealand South Coast - 15/07/2009	x	x	x	x	x
Gizo, Solomon Islands - 02/04/2007	x	x	x	x	x
South Central Chile - 22/05/1960	x	-	-	-	-

Further to this, current meter data was available at the Balls Head current meter located in Sydney Harbour (approximately 200m West of Fort Denison), as well as at 2 separate current metres located just outside of the Port Kembla Outer Harbour. The availability of this data is shown below in Table 7.3. The Balls Head current meter sits in approximately 30m of water and the current data was provided as a depth averaged value over the top 12m of the water column. The Port Kembla current meters each sit in approximately 19m of water and current data was provided for seven different depth bins that are located every 2m in between 3m and 15m depth. The locations of the current meters are presented in Figures 6.1 to 6.4.

Table 7-3: Available Quality Assured Current Meter Data

Tsunami Event	Balls Head (Sydney Harbour)	Botany Bay	Port Kembla Northern	Port Kembla Eastern	Eden
Honshu, Japan - 11/03/2011	x	-	-	x	-
Chile, South America - 27/02/2010	x	-	-	x	-
New Zealand South Coast - 15/07/2009	x	-	x	x	-
Gizo, Solomon Islands - 02/04/2007	x	-	x	-	-
South Central Chile - 22/05/1960	-	-	x	-	-

7.3.2 Quality Assurance of Historical Records

Tide gauge and current meter data from Sydney Harbour, Botany Bay and Port Kembla were collected as part of SPC and PKPC operational met-ocean data collection systems. The main aim of the data collected by these systems is to provide real time data for use during shipping movements and other port operations.

Due to this, water level data was not collected for the purpose of measuring relatively short period tsunami waves, but rather for longer period tides. Tide gauge data was generally collected from instruments with some form of high frequency filter to remove short period waves (for example, a stilling well). A number of

individual water level readings were measured each minute before being averaged into a single value each minute. At some locations individual values were checked before the overall average was calculated. For the purposes of this study, data was further quality checked by extracting the 1 minute records and then manually inspecting plots of the data to determine whether individual 1 minute averaged values were valid.

Current data within the ports is used to detect shorter period events than tsunami and therefore has less high frequency filtering applied to the raw data than the measured water level data. This can make the current data appear noisier than the 1 minute water level data. Current data at Port Kembla is measured at 2Hz before being averaged to produce a 1 minute value while data at Sydney Harbour is measured at 0.5Hz before being averaged to produce a 1 minute value. No data checking is conducted on the individual values used as part of the 1 minute average. For the purposes of this study, data was quality checked by extracting the 1 minute records and manually inspecting plots of the data to determine whether individual 1 minute values were valid.

7.3.3 T2 Scenario Selection

Advice was received from the BoM as to which T2 scenarios were most appropriate to represent each identified event. Determining the appropriateness of these events was not straight forward as the BoM needed to match T2 scenarios to historical events based on event magnitude, location, rupture width and length as well as deep water tsunameter observations. In this way the selection of T2 scenarios was somewhat subjective, as some events could be represented by several different T2 scenarios. In some cases what seemed to be the obvious choice of scenario turned out not to be a good match to the historical event.

As a result, when comparing the results of the validation model runs with corresponding historical records, it is important to take into account that the selected T2 scenarios are merely *representative* of the historical events.

7.3.4 Analysis Methodology

Model runs were then run to simulate these scenarios and the results were analysed and compared to the extracted historical records in terms of tsunami wave height, average tsunami period and spectral energy description.

Consistent methods of analysis were applied to the measured and modelled signals to enable a meaningful comparison between the two to be made. As the T2 scenarios used in the Delft3D modelling were not exact replicas of the recorded events, but rather were a best representation, achieving an exact match with historical records in terms of the tsunami wave train was not feasible. Validation was therefore conducted by comparing a historical record with its Delft3D model with relevant T2 boundary conditions in terms of statistical wave characteristics for a period of 20 hours after the tsunami was first detected inshore.

Output from this analysis is presented in a series of figures contained within Appendix B. The following steps were applied:-

- Raw measured data was re-sampled (and in-filled, where required) to ensure a continuous time-series at 1 minute time steps. Infilling was undertaken using a cubic spline interpolation between valid data points (presented on the top row of Appendix B figures).
- The tsunami signal was isolated by calculating the residual (subtracting the predicted tidal signal) and applying a high pass filter (50% cut-off at 3hours period) to remove any other influences on the signal (such as atmospheric) not associated with tsunami events (presented on the second row of Appendix B figures).
- Model output was extracted at a 1 minute time-step and the simulation start date shifted to the time of the subduction zone earthquake (presented on the third row of Appendix B figures).
- The time of tsunami arrival (for both measured and modelled, separately) was visually estimated using the aid of a low-pass filter with a cut-off frequency (50%) of 15minutes, defined as the first discernible arrival.
- The maximum wave height (or peak current speed) was found by identifying the peak of the signal. The mean wave height was estimated by averaging the peaks over a 20 hour (or length of model output) period following the arrival of the tsunami.
- A spectral density time-series was calculated for both the measured and modelled signals. Spectral analysis (using Fourier Transforms) was completed on sequential overlapping windows of the signals to provide a time varying description of the spectral energy, otherwise known as a spectrogram (presented on the fourth row of Appendix B figures).
- Average 2D energy spectra were calculated over the first 20 hours of the event (or length of model output) (presented on the bottom row of Appendix B figures) to identify the peak period. Spectral moments of the average 2D spectra were then calculated to derive the mean wave period values.

7.3.5 Measured Events

The results of the analyses of the available recorded tsunami data are presented in Appendix B, Table B.1. Upon initial inspection of the results, a number of characteristics were observed.

Figures 7.15 and 7.16 present relationships of rupture magnitude and distance from the tsunamigenic source against recorded wave heights and wave periods. These results suggest that wave heights increase with both rupture magnitude and distance from the tsunamigenic source. However, in the case of the five selected historical events, the larger rupture magnitudes occur at greater distances from the NSW coast and hence the effect of distance from the tsunamigenic source may be biased (it being logical that the further away a source is the more dissipation and dispersion the tsunami will undergo). When considering wave heights originating from Chile it is clear that event magnitude is the dominant cause of increased wave heights (a not unexpected outcome).

Conversely the relationship of wave period to both rupture magnitude and distance from the tsunamigenic source is not as significant. While there is some variation, wave periods tend to be relatively constant across events of different magnitude and source. More importantly perhaps, both Figures 7.15 and 7.16 highlight that the wave height and wave period response to a given event is a site specific feature.

Figures 7.17 to 7.20 plot tsunami wave properties at the tide gauge locations for the five historical events (measured data in the top pane). These plots further confirm that tsunami wave properties are site specific with each site displaying differing responses to the same events. This is likely a result of local factors, such as shoreline shape, bathymetry, size of the embayment and exposure/coastal orientation.

For example, Figure 7.17 shows that the recorded wave height is always larger in the Port Kembla Inner Harbour (most likely due to local resonance) than the Port Kembla Outer Harbour, despite them being connected waterways, and that Fort Denison and Botany Bay have consistently smaller wave heights than the other sites. This may be the result of the Parramatta and Georges Rivers allowing tsunami wave energy to pass through these sites; as opposed to the other sites which are located in enclosed bays/ports. Furthermore, Port Kembla Inner and Outer Harbours show the smallest variance in average period (being potentially governed by resonance), and tended to show shorter wave periods than Botany Bay or Sydney Harbour. Eden Harbour showed consistently longer wave periods than the other sites, perhaps a result of being less enclosed than other sites.

Consistent outcomes such as these, observed over a number of differing events (in terms of offshore magnitude/wave period etc.), suggests that local site specific characteristics are as important as the offshore characteristics (such as tsunamigenic source and magnitude) in producing the observed tsunami signal at a given site. This further emphasises the need to validate the Delft3D model against measured tsunami signals at the study sites.

7.3.6 Validation Outcomes

Numerical modelling results of the historical events are summarised in Tables B.1 and B.2 (Appendix B) with direct comparisons to measured signals also provided in Figures B.1 to B.26 (Appendix B).

Arrival Time

The arrival time of the modelled results depends upon two different stages of tsunami travel. First is the time taken for the tsunami to travel from the rupture location to the D3D model boundaries, located just off the continental shelf (as described in Section 6.4). This travel time is defined by the T2 model simulations, descriptions of which can be found in Greenslade et al. (2011) that describe the excellent agreement of the T2 database with observed records. Travel times to the NSW coast can range from 2 hours for tsunami originating in New Zealand (Puysegur trench) to 14 hours for tsunami resulting from a rupture in South America. From this point tsunami arrival time is dependent upon wave propagation within the local Delft3D models. Table B.1 (Appendix B) shows that the modelled arrival times for tsunami originating in the South Pacific match very well and typically within 10 minutes of the observed arrival time, while tsunami originating from further away, such as Japan and South America tended to show differences in the order of 1 hour.

It should be noted that the determination of the exact arrival time from recorded tide gauge data was not always straight forward. Figures B.1 to B.18 (Appendix B) show that recorded tide gauge signals often possess a certain level of background noise that makes detection of the first tsunami wave somewhat subjective, especially when the first wave is of low amplitude, which is typical of distant tsunami events. The process was aided by application of a low-pass filter to distil the lower frequency tsunami signal.

Wave Heights

In general, modelled wave heights (both maximum and mean) show a good match to historical records and are typically within 20%. The best matches are found from the 2009, 2010 and 2011 tsunami events. Modelled wave heights for the 2007 Solomon Islands tsunami event, were consistently underestimated by the model, which is likely a result of the selected T2 scenario. The 1960 event showed disagreement with the measured Fort Denison data for the event, overestimating wave heights, again most likely due to the T2 scenario selected by the BoM, which had a larger rupture dimension than what is documented for this earthquake. It is important to note that due to the validation model runs being conducted from a still water level, the results will not include any tidal effects. Section 7.4.1 shows that the tide level upon which a tsunami arrives inshore can have a small effect on tsunami wave amplitude.

Spectral Energy

The distribution of energy within the calculated spectra (Appendix B, Figures B.1 to B.18 – bottom two rows of each figure) compares very well between measured and modelled events. Generally, it is found that the frequency band with the predominant energy is the same. This is further confirmed by the comparison of peak wave periods. These comparisons further highlight the site specific response to each tsunami event.

In most cases it is found that the measured data includes some higher frequency energy that is not shown in the modelling. This higher frequency energy could be from reflections and scattering of the tsunami or from other non-tsunami related processes. In any case this higher frequency energy does not significantly affect the observed wave heights and the comparisons to modelled outcomes. It does, however, affect the measures of mean periods where the spectral moments are biased to the higher frequency energy. As such, measured mean wave periods are lower than modelled.

Current Velocities

Table B.2 (Appendix B) presents the outcomes of an analysis of current speeds from both the measured and modelled signals. Comparisons between the two signals for each event are also presented in Figures B.19 to B.26 (Appendix B). While the comparisons are reasonable they are perhaps not as satisfactory as the water level/wave height comparisons. Typically peak current speeds from the modelling are of the correct order of magnitude while the more persistent (mean) current peaks compare well. The distribution of spectral energy along with peak period of the signals compares very well. There are some inherent limitations in comparing depth-averaged model output to high resolution current meter data, predominantly to do with the high frequency 'noise' in the field data. This, however, is not thought to influence the comparisons considerably.

7.3.7 Discussion

The comparisons between modelled and measured signals of historical events indicate that the adopted modelling approach using the Delft3D numerical model with T2 scenarios for water level boundary conditions is capable of replicating what is physically realistic and lends assurance that the results of the inundation modelling can be used with a degree of confidence.

When comparing the Delft3D model results with historical records, there are several factors to consider. Aside from the uncertainty involved in selecting representative T2 scenarios (see Section 7.3.2), it is important to take into account uncertainty within the T2 model scenarios themselves. Greenslade et al. (2009 & 2011) showed that while the T2 database provides a good match to DART II buoys (as good a match as is currently possible/practical) for recorded events, there are still uncertainties in the T2 scenarios, particularly in terms of the number and timing of the maximum peaks in the signal. These uncertainties will in turn affect the validation outcomes, although the extent of that cannot be defined. However, as stated previously local site characteristics can be just as important in producing observed inshore signals.

Additionally, it should be noted that despite the application of quality assurance procedures, there are inherent limitations in tide gauge and current meter data and their application to recording tsunami (for which they are not intended). Higher frequency 'noise', naturally present in the field, cannot be represented by the numerical model forcing and hence influences the presented comparisons.

With the above in mind, it is considered that the numerical modelling approach performs well for the task of simulating tsunami at the study sites in question. The observations of measured signals (in Section 7.3.5) identified that local site specific factors (such as local harbour shape, orientation and bathymetry) influence the observed inshore signal. Figures 7.17 to 7.20 present the summarised modelled results from all events at all sites and demonstrate that, in general, the comparative and relative response of each site between events is replicated by the model.

7.4 Model Sensitivity

The model was tested for sensitivity for the following elements:-

- Tidal interactions;
- Seabed roughness;
- Overland roughness;
- Grid resolution;
- Simulation Run Time; and
- Coastal Structures Schematisation.

7.4.1 Tidal Interactions

One aspect of the tsunami modelling within this project involves the investigation of inundation at different tidal levels and phasing. As such it was necessary to examine the effects of the tidal-tsunami interactions – tide level and interaction with the tidal currents. As some of the tsunami simulations were conducted at mean sea level (MSL), several tests were conducted into the effects of tsunami arrival coinciding with MSL on a rising and falling tide. Furthermore, the effect of high water on tsunami wave heights was considered. Outcomes from this series of test simulations are provided in Figure 7.21. Note that the individual time series were post-processed to synchronise the highest tsunami wave of each simulation with that of the HAT simulation. The same shift was adopted for the speed and water level plots.

When MSL occurs on a falling tide, tidal flows are heading out to sea and thus oppose the propagation of the

tsunami. Whilst this reduces the tsunami velocity, it also causes some additional wave shoaling and results in higher tsunami wave heights. This is a common phenomenon in wave-current interactions. Conversely, when the MSL occurred on a rising tide, tidal velocities and tsunami velocities complemented each other and the tsunami velocity increased. The influence of tidal currents will be site specific and may also have an effect on the direction of tsunami propagation. Note, however, that the highest tsunami speeds do not necessarily occur during the greatest trough to crest water level variation. The water levels were not de-trended for tidal level variation (i.e. the tidal signal was not removed) over the 130 minutes of results presented in Figure 7.21.

Tsunami arriving at a high tide (HAT) resulted in tsunami wave heights that were smaller when compared to tsunami arriving at MSL (in the order of 5-12% - see Figure 7.21). This is because when arriving at HAT, a tsunami is in deeper water, and hence less shoaling has taken place when compared to tsunami arriving at MSL at the same location – although still resulting in higher water levels.

The outcomes of these tidal investigations have demonstrated that tides have an influence on the propagation of tsunami in the nearshore region and hence confirm the need for an approach of investigating inundation at different tidal phases within the design simulations.

7.4.2 Seabed Roughness

The sensitivity of tsunami propagation to the adopted seabed roughness parameter was investigated through a series of simulations that applied a range of Manning's roughness coefficients (Manning's n = 0.015, 0.02 and 0.03). The results of these investigations are presented in Figures 7.22A and 7.22B. They show that any variation within the physically realistic range of Manning values has negligible effect of the inshore tsunami wave height, velocities and directions and hence a value of 0.020 was used, in line with the outcomes of the tidal calibration (see Section 7.1).

7.4.3 Overland Roughness

The propagation of tsunami over the shoreline and coastal land areas will be heavily influenced by the model roughness parameter that is adopted for the land (Section 6.3). As in overland flow studies, the model roughness is a very important and spatially variable parameter that dominates the hydraulic solution (as opposed to viscosity terms in coastal/oceanographic settings) and must be given careful consideration in order to accurately determine the inundation extent and associated hazard from tsunami. Unlike nearshore swell wave run-up and overtopping, tsunami may propagate kilometres inland, thereby increasing the influence of roughness on the propagation of the waves. This effect is compounded by the retained water from preceding waves that provide deeper water for on-land propagation.

In order to investigate the effect and sensitivity of these roughness parameters, a 'numerical flume' model that described a smaller sample area was developed over a section of the Lake Macquarie study area. The flume consisted of a 200m wide grid domain that extended from the offshore boundary of the overall model up to the +15mAHD contour. Initially a fine 2m grid resolution over the foreshore areas was established that described impermeable physical structures such as buildings (based on cadastral and aerial image information) as raised structures and then determining the extent of the flow through that area during a tsunami.

Delft3D is able to include a spatially variable roughness grid that can be utilised to define the range of land characteristics such as roads, residential properties and parklands. Utilising this feature the flume model was run again with the physical structures removed, and instead replaced by a spatially variable roughness grid which contained a range of roughness values to describe different types of land. A comparison of the extents is presented in Figure 7.23. A similar method was used by Gayer et al (2010).

From these results it was possible to determine which combination of roughness values provided a flow extent that most closely resembled the flow extent obtained when physical structures were present. In this way Cardno was able to derive a suitable roughness parameter for each land type. These values are summarised in Table 7.4 and their application demonstrated in Figure 7.24.

Table 7-4: Adopted Overland Roughness Values

Land Usage	Manning Roughness Value (n)
Road	0.02
Residential/Commercial	0.10
Parkland/Forrest	0.07
Open Grassland	0.03

Furthermore, in testing the sensitivity of the model to various roughness parameters, it was possible to ascertain a measure of the reliability of the model and inundation outcomes.

7.4.4 Grid Resolution

Once the appropriate roughness parameters were determined it was also necessary to determine the effect of the size of the grid resolution. Whilst a grid resolution of 1m to 2m would describe the land areas with great detail and provide highly detailed results, numerical modelling at this refinement can be computationally demanding and time consuming when large areas need to be investigated. Thus it was necessary to determine a grid resolution that not only described the results with similar levels of accuracy, but would also allow for reasonable model run times.

To this end a series of flume runs were conducted, this time testing a two different grid refinements, 2m and 10m. The resulting inundation extents for these grid refinements are presented in Figure 7.25. From these outcomes it is considered that a 10m grid cell resolution, together with the specified bed friction parameter values, adequately describes the spatial variability and extent of the inundation and provides for significantly reduced simulation times. Hence it was deemed a far more practical grid resolution alternative.

7.4.5 Simulation Run Time

Due to the highly complex interactions of tsunami over the continental shelf and nearshore zone, the peak wave height within a given event may occur many hours after the arrival of the first wave. Boundary conditions applied to the inundation model, extracted from the T2 database, are 24 hour time series from the

time of initial rupture. Subduction zones such as Puysegur, Tonga, New Hebrides and Kermadec all lie within a travel time of roughly 2-6 hours, meaning that there was 18-22 hours of boundary conditions data following the arrival of the first wave at the study sites. For events from South America, travel times are between 12-15 hours, which limits the effective simulation time at each site. Following discussions with the BoM, T2 scenarios from these distant sources were re-modelled and 36 hour (from time of rupture) time series supplied for this study. However, due to the significant number of model runs within this assessment, it was necessary to select a model run time that not only described all significant features of the tsunami event, but also allowed for economical run times.

To this end, a sensitivity run was undertaken to investigate the potential for large tsunami waves occurring more than 12 hours after initial arrival of the tsunami at the study sites. The outcomes of this sensitivity simulation, presented in Figure 7.26, shows that while some significant waves do occur, the peak of the event typically occurred within the first 6 hours, hence model run times were kept consistent with the boundary condition time series for each event.

7.4.6 Model Schematisation of Coastal Structures

At a number of the study sites, permanent coastal structures exist that would significantly affect the nature and scale of inundation of the foreshore areas. It is therefore imperative to ensure that these structures are adequately described by the models. Delft3D has the capability of implementing sub-grid scale structures/features such as weirs, which are specified as fixed non-movable constructions generating energy losses due to constriction of flow. They are commonly used to model sudden changes in depth such as seawalls, cliffs and groynes in simulations. However, implementation of these structures requires detailed information of crest levels and dimensions. Given the high resolution model grid and underlying LiDAR data, it was considered that the bathymetric description of the model grid would be adequate in describing these foreshore features.

To test this assumption the sensitivity of using sub-grid scale structures was investigated by implementing a 2D weir structure and comparing the outcome of a large inundation event to an outcome where foreshore crest levels are defined with the model bathymetry alone. Manly was chosen as the testing site, as there exists a substantial seawall structure along its beach front. Furthermore, previous work at Manly meant that Cardno had previous knowledge of the constructed levels of this structure.

A 10,000 years ARI event from New Hebrides was chosen as the scenario to test, being a significant inundation event, and hence any effects of the seawall would be highlighted. The sensitivity of the inundation outcome to the definition of the seawall structure is presented in Figure 7.27 and shows negligible difference in the ultimate inundation extent. From this it can be concluded that the grid/bathymetry adequately describes the seawall and in particular its crest levels. This is due to the fact that the grid is of high enough resolution and during model setup, it was ensured that crest levels of the seawall were correctly described. Such an approach was applied to all study sites. Furthermore, when defining depths the numerical scheme of the model applies the maximum depth of the surrounding grid points, hence large steps in bathymetry (e.g. seawalls, cliffs) were inherently described as such.

8 TSUNAMI MODELLING

The following section provides a reference to the full suite of tsunami scenarios and simulation outputs produced in this study.

8.1 Tsunami Scenarios

The selection of modelled scenarios has been discussed and presented within Sections 4.2, 4.3 and Appendix A. The subduction zones identified through the selection process represent sources that generate tsunami of a range of approaching directions and alignments to each of the NSW coastal study sites (Section 1.2). This ensures that any localised sensitivities at each study site are included in the investigation.

Table 8.1 summarises the 24 simulations that were completed for each of the five study sites. While the set of critical source zones (subduction zones) is the same at each of the five study sites, the individual events simulated from these zones are unique for each study site (as discussed in Section 4.3).

Table 8-1: Summary List of Modelled Tsunami Scenarios at Each Location

Scenario No.	ARI (years)	Source Zone *	Water Level ^	Scenario No.	ARI (years)	Source Zone *	Water Level ^
S1	200	KER	HAT	S13	2000	KER	HAT
S2	200	NHB	HAT	S14	2000	NHB	HAT
S3	200	PUY	HAT	S15	2000	PUY	HAT
S4	200	SCH	HAT	S16	2000	KER	MSL
S5	200	TGA	HAT	S17	2000	NHB	MSL
S6	500	KER	HAT	S18	2000	PUY	MSL
S7	500	NHB	HAT	S19	5000	NHB	HAT
S8	500	PUY	HAT	S20	5000	PUY	HAT
S9	500	TGA	HAT	S21	5000	NHB	MSL
S10	1000	KER	HAT	S22	5000	PUY	MSL
S11	1000	NHB	HAT	S23	10000	NHB	HAT
S12	1000	PUY	HAT	S24	10000	PUY	HAT

* KER = Kermadec, NHB = New Hebrides, PUY = Puysegur, SCH = South Chile, TGA = Tonga

^ HAT = Highest Astronomical Tide, MSL = Mean Sea Level

8.2 Scenario Results and Output

Summary results from the scenario modelling are provided in Appendix C as the peak tsunami wave heights at the 100, 20 and 5m depth contours as well as the maximum run-up levels. Furthermore, it is intended that output from the inundation modelling can be used in future detailed risk assessments at each of the study sites and hence detailed output from the inundation modelling includes the following:-

- Water Level
- Inundation Depth (D)
- Extent of Inundation
- Duration of Inundation
- Velocity (V); and
- Hydraulic Hazard (V x D).

The maximum value over the duration of the model simulation was mapped at each spatial grid point for each of the above listed parameters. Time-series plots for selected parameters were also extracted from the model simulations. Both sets of output are provided at the five study sites for all scenarios in Appendix D. Due to the large number of output figures, Appendix D is provided as an electronic appendix to this report. Extent mapping has also been provided in GIS format to the NSW SES, OEH and BoM to allow comparison with and assessment of the existing tsunami emergency response protocols.

8.2.1 Boundary Condition Verification

Given the adopted approach to scenario selection (Tsu-DAT) and application of boundary conditions (T2), it is important to ensure that the boundary conditions applied provide the intended near shore tsunami wave heights. Figure 8.1 provides a scatter plot that compares the outcomes of the D3D modelling with the Tsu-DAT wave heights at the 100m water depth contour. Tsunami wave heights from the detailed D3D modelling matched those of Tsu-DAT at the 100m depth contour to within 15%, which is in the same order of magnitude as the confidence limits of the recurrence interval output from Tsu-DAT.

Due to the complex interactions between tsunami and the bathymetric details in the near shore zone, as well as the variability of responses to differing source zones, it was observed that in certain instances a tsunami of lower wave height at the 100m contour, actually produced a larger inshore tsunami wave height (and overland run-up) than a tsunami of higher wave height at the 100m contour. Such an outcome is observed at the Swansea study site, where the 1000-years ARI inshore wave height at the 5m depth contour from the Puysegur subduction zone (Scenario 12) is larger than the 2000-years ARI wave height from the New Hebrides subduction zone (Scenario 14). Figures 8.2 to 8.4 plot ARI level against tsunami amplitude at the 100m contour, and show that such an outcome is not common. With this in mind, it is important to note that the wave height at a particular ARI level at the 100m contour will not necessarily produce overland run-up of the same ARI level. However, given the available probabilistic information of tsunami wave heights on which this study is based, and the presentation of ARI outcomes as envelope results (Section 9), such occurrences are tolerated.

8.3 Discussion

Swansea

Based on the inundation extents, Swansea appears to be the site most exposed to tsunami, in terms of number of properties inundated. South of the Swansea Channel, the most severely affected areas lie near Channel Street and the Burragallana Reserve (see Figure 8.5), as well as Chalmers and Bridge Streets to the east of the Swansea Bridge. At higher ARIs (up to 5000 years, almost all of Swansea, north of Milray Street, undergoes some kind of inundation, from the Swansea channel in the east overland to Lake Macquarie in the west. Areas directly to the south of the Lake Entrance such as Northcote Avenue and Bowman Street are also affected, with areas further south protected by their elevated topography. Minimal inundation occurs around the Swansea Heads region due to its higher elevation.

North of the Swansea Channel, inundation from lower ARI events occurs from the south, at the Swansea channel entrance, as opposed to inundation from the east (ocean). This is due to the elevated topography of the dunes at the back of Blacksmiths Beach. As a result of this the most severely affected areas are Bali Street and Ungala Road, and the adjacent area several hundred metres to the north. The raised embankment of the old Pacific Highway appears to offer some protection to the areas to the west of it for lower ARI cases. At the 10,000-years ARI, most of the area to the south of Belmont lagoon undergoes inundation, with the exception of the elevated areas around Marks Point and Belmont Park.

Manly

The Manly study site had the second highest run-up level of all the modelled sites. Manly Corso is affected by inundation from tsunami waves coming from not only the open ocean to the east, but also from Manly Cove to the west (see Figure 8.6). The results of the modelling indicated that very little if any attenuation of peak water level occurs as the tsunami waves refract around North Head. Areas affected by inundation are generally the Corso, north of the Corso along Manly Beach, as well as some areas near Manly Lagoon and its surrounding reserves. Most areas to the south of Ashburner St are protected by the elevated topography of North Head.

The most severe inundation occurs from Ashburner Street north to the Corso. Here initial inundation occurs from Manly Cove at ARI levels of 500 years or higher (affecting land to the south of Victor Parade West), with 2000 years appearing to be the threshold of severe inundation. North of the Corso and along Manly Beach, the elevated terrain means that inundation only occurs inland of the back beach for 5000-years ARI or higher. The 10,000-years ARI inundation extends west to Manly Oval (some 400m inland), Kangaroo Street, and Pine Lane to the north. North of here, around Manly lagoon, low lying areas are affected by tsunami of 1000-years ARI and higher, with the majority of inundation affecting Manly Golf Course and Passmore and Nolan Reserves.

Botany Bay

Botany Bay has the lowest run-up level of any of the study sites. This is due to the relatively small entrance that restricts penetration of the tsunami into the Bay, from which point the tsunami energy reduces across the wide embayment as a result of refraction/diffraction. The most severe inundation occurs around Kurnell,

mostly due to its low lying topography, whilst other areas affected by inundation (albeit less severely) include Banksmeadow, Botany and Kyeemagh, which is also inundated from behind via the Cooks River (see Figures 8.7 and 8.8).

The area of Kurnell west of Balboa Street is inundated at recurrence levels of 200 years. At the 500-years ARI level, most of Prince Charles Parade and its surrounding properties become inundated. For 10,000-years ARI events, most of Kurnell west of Dampier Street and north of Torres Street is affected by inundation. Around Botany, to the east of the airport runways, most inundation occurs south of Bay Street and west of Botany Road, with Foreshore Road affected south to Banksmeadow. Furthermore, low lying areas adjacent to Muddy Creek and Kyeemagh are affected at the higher ARI levels.

Wollongong / Port Kembla

Wollongong seems to be the most well protected site from low ARI events, mainly due to the pronounced dune system along the length of the study site. The two main areas of inundation for Wollongong sit in the low lying areas near Wollongong Harbour and Para Creek (see Figures 8.9 and 8.10). At Wollongong Harbour both breakwaters (including the base of Wollongong Lighthouse and the Harbour Front wharf and car park) are affected by low ARI events, due to the funnelling of tsunami wave energy through the Wollongong Harbour Entrance. However, the inundation does not extend inland over Cliff Road or Grand Pacific Drive until at least the 2000-years ARI level. At these less frequent recurrence levels, inundation extends over Osborne Park and for the 10,000-years ARI events extends past Wilson Street. Flagstaff Hill remains unaffected due to its high elevation. Around Para Creek, inundation occurs past the 1000-years ARI threshold. Above this threshold, inundation occurs particularly around Achilles Avenue, Exeter and Montague Streets. Furthermore, low lying areas around the Squires Way Bridge and Stuart Park also would suffer from significant inundation.

South of Wollongong Harbour around Coniston Beach, very little inundation runs up past the back beach dunes until the 2000-years ARI threshold. Here inundation only occurs south of WIN stadium, over Wollongong Golf Course. For 10,000-years ARI events, inundation in this area is extensive, running inland over the Golf Course past Corrimal Street, even as far as Evans Street. This significant inundation occurs as far south as the Sewage Treatment works.

Around Port Kembla, the south of the outer harbour is affected by inundation from 200-years ARI events, with areas around Foreshore Road particularly affected. For higher ARIs inundation generally extends (from the outer harbour) inland past Darcy Road and even Port Kembla railway station and its surrounding railway lines. Around the inner harbour, areas most heavily affected by inundation include areas around the northern wharf and Gurungaty Waterway.

Merimbula

Merimbula has the least number of properties affected of any site, mainly due to its small size and high proportion of elevated land. This said, there are still areas of significant inundation at even 200-years ARI. Areas to the south of the waterway, particularly Fishpen Road, Burton Avenue and Marine Parade all incur inundation at the 200-years ARI events (see Figure 8.11). Note that at lower ARI levels this area is protected

from inundation from the east by the high elevation of the dunes at main beach and as such inundation occurs after waves pass into the entrance of Merimbula Harbour and refract around towards the bridge.

For the less frequent ARIs, the entire populated areas south of the harbour would suffer from inundation, as run-up begins to run over the aforementioned main beach dunes. The outskirts of Merimbula Airport become inundated at the lower ARI events, but the runway itself and part of Arthur Kaine Drive are not subject to inundation until the 5000-years ARI threshold.

North of Merimbula Harbour, most of the inundation occurs in the low lying areas east of Market Street, predominantly Beach Street and then further to the north, Main Street. For higher ARI events, inundation extends as far inland as the western edge of Park Street. It should be noted that some inundation occurs to the low lying areas surrounding Back Lake, even inundating Berrambool Sport Ground, but most of the inundated area could be classified as uninhabited park land. Some properties off Berrambool Drive and Garden Circle may be affected. For 10,000-years ARI events, inundation connects Back Lake with Merimbula Harbour via Randolph and Henwood Streets.

8.4 Inundation Thresholds

An objective of this study was to identify at each site whether a threshold in the range of tsunami events/magnitudes exists where in broad qualitative terms a significant increase in land inundation occurs giving consideration to inundation and potential impacts on urban areas as well as public, private and critical infrastructure sites.

All simulated scenarios produce some inundation above the adopted still water (tide) level, and hence specifying a threshold based on tsunami run-up exceeding a given level is somewhat arbitrary. Furthermore, run-up levels are highly variable at a given site. One parameter that provides a useful measure on the nature of any inundation is hydraulic hazard (V x D). This parameter was mapped for each modelled scenario (Appendix D).

It is then possible to calculate the area that is subject to a particular hazard level to gauge whether there is a particular threshold at which significant inundation occurs. To do this a hazard level of 1.0 (in line with Appendix L of the NSW Floodplain Development Manual) was investigated and the percentage area of habitable land within each study area that exceeded this hazard level was calculated.

A qualitative assessment of such analysis suggests that the threshold for significant inundation (defined nominally as 2% of the habitable area within the 1.0 hazard extent) is between the 1000 and 2000-years ARI levels for four of the study sites, while for Manly this threshold is between the 500 and 1000-years ARI levels. These outcomes are consistent with the existing Joint Australian Tsunami Warning Centre system as presented by Uslu and Greenslade (2012), which found similar thresholds for the issuance of land warnings at the five study sites.

8.5 Tsunami Arrival Times

Arrival times for the tsunami simulations are a consequence of the distance a tsunami wave has to travel from source to landfall, and the forward speed of the tsunami wave train (a result of the ocean depth – described in Section 2.2). Table 8.2 provides tsunami arrival time for the 120 simulations, where arrival time is defined as the total time from rupture to the first noticeable deviation from predicted tide at the study site. In this instance a threshold of 0.5cm deviation was instituted as a "noticeable" deviation.

Table 8-2: Summary List of Modelled Tsunami Scenario Arrival Times

ARI	SOURCE	TIDE	Tsunami Arrival Time (hours)				
			Site				
			LMQ	MLY	BBY	WPK	MBA
200	KER	HAT	04:37	04:36	04:36	04:41	04:46
200	NHB	HAT	03:50	03:54	03:56	04:14	04:18
200	PUY	HAT	02:40	02:38	02:34	02:31	02:27
200	SCH	HAT	14:04	14:02	14:00	13:57	13:41
200	TGA	HAT	05:15	05:21	05:23	05:40	05:48
500	KER	HAT	04:35	04:33	04:34	04:39	04:44
500	NHB	HAT	03:46	03:49	03:51	04:00	04:15
500	PUY	HAT	02:31	02:31	02:31	02:27	02:20
500	TGA	HAT	05:09	05:10	05:10	05:17	05:32
1000	KER	HAT	04:33	04:32	04:34	04:38	04:43
1000	NHB	HAT	03:44	03:48	03:50	03:57	04:12
1000	PUY	HAT	02:29	02:29	02:28	02:27	02:19
2000	KER	HAT	04:32	04:31	04:33	04:37	04:42
2000	NHB	HAT	03:43	03:46	03:48	03:56	04:11
2000	PUY	HAT	02:29	02:27	02:27	02:26	02:18
2000	KER	MSL	04:32	04:31	04:33	04:37	04:42
2000	NHB	MSL	03:43	03:46	03:48	03:56	04:11
2000	PUY	MSL	02:29	02:27	02:27	02:26	02:18
5000	NHB	HAT	03:42	03:44	03:47	03:54	04:10
5000	PUY	HAT	02:28	02:27	02:26	02:26	02:17
5000	NHB	MSL	03:42	03:44	03:47	03:54	04:10
5000	PUY	MSL	02:28	02:27	02:26	02:26	02:17
10000	NHB	HAT	03:40	03:43	03:46	03:52	04:09
10000	PUY	HAT	02:28	02:26	02:26	02:25	02:17

Whilst arrival times did not vary significantly with increasing ARI, the higher ARI scenarios did have slightly earlier arrival times than their lower ARI equivalents. This can be attributed to the fact that tsunami wave trains with larger wave amplitudes crossed the "noticeable" deviation threshold slightly sooner. In order to give representative arrival time values for source zone – study site combinations, arrival times were averaged across the ARI spectrum, with the results given in Table 8.3. The results show that the Puysegur source zone

is the most critical from an emergency management perspective with arrival time in the vicinity of two and a half hours for all of the sites, while tsunami from South Chile take approximately 14 hours to reach the NSW coastline.

Table 8-3: Summary List of Average Modelled Tsunami Scenario Arrival Times

SOURCE	Average Tsunami Arrival Time (hours)				
	Site				
	LMQ	MLY	BBY	WPK	MBA
KER	04:34	04:33	04:34	04:39	04:44
NHB	03:44	03:47	03:49	03:58	04:12
PUY	02:30	02:29	02:28	02:27	02:19
SCH	14:04	14:02	14:00	13:57	13:41
TGA	05:12	05:16	05:16	05:29	05:40

8.6 Tidal Phasing

Scenarios at the 2000 and 5000-years recurrence levels were run at two tidal levels, HAT and MSL. Comparison of these scenarios allowed for an analysis of the influence of tidal level/phasing on the propagation of tsunami. Inspection of the results shows that the near shore shoaling of the tsunami is comparable between the two water level phasings and not significantly affected by the tide level. This is demonstrated in Figure 8.12, which plots the wave height (i.e. excluding tide level) of the MSL scenarios against the corresponding HAT scenarios. A 1:1 relationship is observed, indicating that the shoaling of the tsunami wave height is not sensitive to the tidal phasing at the 5m contour.

However, maximum crest level (i.e. including tide level) will be dependent on the phase of the tide; crest level being a summation of the wave amplitude (tsunami wave height) and the tide level at a particular time. In fact the results of some MSL simulations produce a larger crest level than the equivalent HAT simulations (e.g. 5000-years ARI event from Puysegur at Swansea, or 2000-years ARI event from Kermadec at Merimbula – see Figure 8.13).

As described in Section 6.5.2 the desired tidal phasing for each scenario was selected to correspond to the arrival of the maximum wave height. However, for MSL scenarios where a large wave height occurs some 6 hours after the arrival of the maximum wave, it will correspond to a high tide level and as a result may produce the maximum crest level of the event.

8.7 Estuary Response

The selected study sites allowed for a limited review of how tsunami respond within estuaries and coastal rivers. A number of such coastal features were present within the study sites. These include Lake Macquarie, Sydney Harbour, Botany Bay and Merimbula Lake. A particular feature of these estuarine systems is that the width of the entrance is small in relation to the width of the estuary or length of the coastal river. As a result, the tsunami waves within these estuarine embayments are refracted/diffracted and the peak wave height reduces as the tsunami propagates along the estuary/coastal river.

Figures 8.14 and 8.15 present spatial plots of maximum water levels for a 10,000-years ARI event within the Parramatta River (Sydney Harbour) and Botany Bay/Georges River systems. The nature of tsunami attenuation within these systems is evident from the maximum water level plots, however, localised, responses resulting in higher wave heights within small embayments are observed. Through the main body/channel of the systems the maximum wave height reduces with distance from the entrance; however, small embayments off the main tributary show resonant responses.

Overall, the maximum water level figures depict a complex response of estuarine systems to tsunami that is heavily influenced by localised shoreline shapes/features. The existing model setups are not adequate (in terms of grid resolution and bathymetry) to properly investigate these responses as these features lie outside the focus areas of the study sites.

9 COASTAL RISK ASSESSMENT

The coastal risk assessment aims to inform the identification of low-lying areas of the NSW coast that are particularly vulnerable to tsunami inundation. To do so, the outcomes of this study have been directed more towards investigating land threat inundation events and this is aimed at informing the higher level emergency response planning that is required to deal with the likely catastrophic consequences of tsunami inundation.

The following assessment is intended to build on and refine the preliminary risk assessment undertaken in Stage 1 of the NSW Tsunami Risk Assessment (Risk Frontiers and URS, 2008). Detailed risk assessments typically consider two aspects, being probability (likelihood) and magnitude of potential loss (consequence). While probability is addressed in the current work no detailed investigation of the magnitude of potential loss is undertaken but rather outputs from the inundation modelling (see Section 8 and Appendix D) are presented in such a way as to allow such a detailed assessment to be made in the future.

Inundation modelling was undertaken using a pseudo-probabilistic approach. That is, multiple tsunami scenarios have been considered, and an assessment of the vulnerability of the coastal area to tsunami hazard can now be evaluated. It is important to note that more extreme outcomes than those presented in this report are possible, but would be of particularly low probability.

9.1 Inundation Extents

To provide a summary of the inundation threat at each study location envelope extents at each ARI level are provided in Figures 9.1 to 9.5. These are derived by taking the maximum water level/depth output from all individual simulations at a given ARI level. While the envelope extents are presented for specific ARI levels it must be noted that recurrence of each tsunami event is assessed at the 100m water depth location (taken from Tsu-DAT). Due to complex nearshore processes (that is, scattering of the tsunami signal as it interacts with the nearshore seabed and coastline as a result of shoaling, refraction and reflection), the recurrence level at the 100m water depth is not the exact recurrence level of the inundation extent, however it can be considered indicative.

9.2 Vulnerability to Tsunami Inundation

Using the envelope extents (Figure 9.1 to 9.5) a measure of the exposure of each study site can be made. This is summarised in Table 9.1 as the number of cadastral lots exposed to inundation at a given ARI level. Using GIS analysis, a cadastral lot was considered to be exposed if an inundation extent overlaid any part of its area. Calculated exposure is provided within postcode boundaries, consistent with the presentation of exposure in the Stage 1 Risk Assessment (Risk Frontiers and URS, 2008).

Table 9-1: Calculated Exposure (by Cadastral Lot) based ARI extent mapping

ARI	Post Code							
	2281	2095	2231	2230	2500	2505	2548	2549
	Reference							
	Swansea	Manly	Kurnell	Cronulla	Wollongong	Port Kembla	Merimbula	Pambula
200	713	150	165	323	30	26	122	6
500	1233	173	262	396	31	27	199	7
1000	1988	261	375	515	49	28	228	8
2000	2502	456	469	573	85	38	300	18
5000	2986	744	653	806	173	42	328	22
10000	3128	1187	716	911	480	80	432	46

In order to provide a direct comparison with Stage 1 Risk Assessment (Risk Frontiers and URS, 2008), the Geo-coded Urban and Rural Addressing System (GURAS) database was interrogated, once again using the envelope inundation extents mentioned in Section 9.1. This is summarised in Table 9.2 as the number of GURAS address points exposed to inundation at a given ARI level. It is important to note that in the GURAS database addresses are given as single point coordinates (usually located in the centre of the corresponding cadastral lot). As a result, addresses considered inundated in the cadastral assessment may not necessarily be considered inundated in the GURAS assessment if the inundation extent only overlaid part of its cadastral area.

Table 9-2: Calculated Exposure (by GURAS entry) based ARI extent mapping

ARI	Post Code							
	2281	2095	2231	2230	2500	2505	2548	2549
	Reference							
	Swansea	Manly	Kurnell	Cronulla	Wollongong	Port Kembla	Merimbula	Pambula
200	428	100	68	386	0	3	80	1
500	1158	262	97	476	0	4	369	1
1000	2121	479	236	625	12	7	465	1
2000	2974	1867	321	836	74	7	667	4
5000	3956	4686	485	1884	259	7	738	5
10000	4271	8515	556	2630	943	8	1179	8

With detailed Stage 2 modelling and hazard mapping completed (Section 8), it was then possible to ground truth the Stage 1 site exposure methodology to inform the assessment of other coastal locations.

It was found that the outcomes of the detailed inundation modelling did not correlate to the assumptions made in the Stage 1 assessment. Outcomes from the Stage 1 study pertaining to the current five study sites are summarised and compared in Table 9.2 (at the ≈500-years ARI level). It is shown that the Stage 1 assessment significantly overestimates the number of affected cadastral lots. Furthermore, the relative exposure of each suburb is not consistent, that is, the exposure ranking of each site is different between

Stage 1 and 2.

Table 9-3: Comparison of Estimated Stage 1 against Calculated Stage 2 Exposure (by GURAS database at the ≈500-years ARI level)

Post Code	Reference	Stage 1 - Broad Based Vulnerability *	Stage 2 - Detailed Inundation Modelling
2281	Swansea	7412	1158
2095	Manly	13839	262
2231	Kurnell	995	97
2230	Cronulla	18952	476
2500	Wollongong	-	0
2505	Port Kembla	-	7
2548	Merimbula	6009	369
2549	Pambula	2000	1

* Summarised from Tables 20 & 21 in Risk Frontiers and URS (2008).

The particular outcomes from the two stages disagree in the following ways:

Nearshore Tsunami Wave Heights

The Stage 1 assessment utilised probabilistic tsunami wave amplitudes (wave heights) estimated by Thio and Somerville (2006), which differed greatly from tsunami wave heights derived using the Tsu-DAT (GA) and T2 (BoM) databases. A comparison of the estimated wave heights is provided below (Table 9.3) and shows that the estimates from Thio and Somerville (2006) are significantly lower than the Tsu-DAT and T2 outcomes. Section 4 of the Stage 1 Assessment (Risk Frontiers and URS, 2008) discusses the differences in near shore tsunami estimates between the Thio and Somerville (2006) and Burbidge et.al. (2008) (on which Tsu-DAT is based), and hypothesises that it is likely due to the assumed maximum magnitudes of subduction zone earthquakes, particularly along the Tonga-Kermadec trench. No further discussion is attempted here, other than to say that the current study relies on the Tsu-DAT (i.e. Burbidge et.al. (2008)) assessment of tsunami risk and in the context of available data can be considered a conservative estimate of near shore tsunami risk, and hence appropriate for emergency response planning.

Table 9-4: Comparison of Stage 1 and Stage 2 Tsunami Wave Heights (m)

	Stage 1 @ 15m depth *			Stage 2 @ 20m depth ^		
Location	475yrARI	975yrARI	10000yrARI	500yrARI	1000yrARI	10000yrARI
Swansea	0.73	0.91	0.99	1.56	2.26	5.74
Manly / Kurnell / Cronulla	0.79	0.86	1.37	1.33	1.91	4.47
Merimbula	0.80	0.94	1.37	2.04	2.33	5.12

* Stage 1 Thio and Somerville (2006).
^ maximum of scenarios at each ARI level from detailed hydrodynamic modelling described in Section 8.

Tsunami Run-up Factors

The broad-based assessment of tsunami vulnerability utilised outcomes from generalised run-up modelling undertaken by Baldock et al. (2008). In that study, tsunami run-up was estimated for a range of generic bay shapes with sensitivities completed for a range of tsunami wave types, periods and seabed slopes. Tsunami run-up factors of between 1 and 6 times the wave height at 20m water depth were derived. For large scale bays (as defined in Baldock 2008) which are more comparable in dimension to the embayment characteristics of the selected Stage 2 study sites, the largest run-up factors were observed within V-shaped and circular-shaped bays.

When compared to equivalent tsunami run-up factors calculated from the detailed inundation modelling (Section 8), it was found that the adopted run-up factors in the Stage 1 assessment significantly overestimate the magnitude of run-up/inundation. Run-up factors calculated from the Stage 2 modelling ranged between 1.0 and 1.7 (wave height at 20m depth / maximum run-up height see Appendix C). This is likely accounted-for by the actual nature of inundation over complex, low-lying foreshore areas and the dimension of the bays/estuaries being considered.

Once run-up of low-lying foreshore areas around the bay is initiated, the resulting inundation is heavily affected by the terrain and frictional losses. In much the same way as wave breaking was found to limit the amplification of the tsunami wave in the work of Baldock et al. (2008), inundation of foreshore areas dissipates the incoming tsunami energy through breaking while also providing flood storage area. This characteristic is not considered in the generalised run-up modelling where vertical, infinitely high, fully reflective walls are assumed, which act to propagate the incoming tsunami energy further into the model domain, thereby maximising run-up factors. Furthermore, the larger run-up factors were derived from V-shaped and circular-shaped bays where narrowing of the embayment causes significant focussing of the incoming tsunami wave.

Baldock et al. (2008) also investigated embayment shapes where the entrance is the same width or of a larger width than the bay and the bathymetry is specified as a constant linear slope. This results in a funnelling of the energy and hence large shoaling/run-up of the tsunami. While these generic shapes are broadly consistent with the sections of each study sites exposed to the open coast, the estuaries investigated within this study (Botany Bay, Sydney Harbour, Merimbula Lake, Lake Macquarie) have smaller entrance widths than the associated bay and/or are much longer than the entrance width, with relatively constant bathymetry. Thus the entrance acts as a constriction to incoming tsunami. As a result the tsunami energy within these estuary embayments is more dispersive and inundation of surrounding lands reduced as a consequence.

It can therefore be inferred that the modelling of generic bay shapes does not adequately account for the influence of highly complex shoreline features and foreshore inundation when deriving run-up factors. An attempt was therefore made to define the run-up factor based on the Stage 2 detailed modelling results, and is discussed in Section 9.4, below.

Property Identification

The vulnerability of particular coastal locations was ranked within the Stage 1 assessment by counting the number of properties below the estimated tsunami run-up level within the postcode/suburb areas. Disregarding differences in the estimated wave height and run-up levels between the two Stages of the risk assessment, total counts of properties did not correlate, that is, in some cases a much greater number of properties were identified at lower run-up levels within the Stage 1 assessment. This is likely a result of the underlying topography used to map the extents of the estimated tsunami run-up cases and the cadastral information used. Where available, the Stage 2 inundation modelling utilised high resolution LiDAR data and utilised cadastral lot areas, hence is considered to be of greater accuracy.

9.3 Proposed Methodology for Tsunami Vulnerability Assessment

In light of the differences outlined above, refinements to the underlying assumptions of the Stage 1 methodology are proposed in order to re-assess the method of broad-based assessment of exposure to tsunami and to redefine the vulnerability rankings to inform the selection of sites for future detailed inundation modelling campaigns. It is intended that the general methodology adopted in the Stage 1 assessment be maintained, as follows:-

- Compile DTMs and identify coastal locations (based on suburb boundaries) that are potentially at risk from tsunami inundation.
- Define probabilistic near shore tsunami amplitudes.
- Estimate average tsunami run-up level.
- Cadastral count based on estimated average tsunami run-up level at a selected ARI level.

Sources of data available to inform such an assessment include topographic data, cadastral information and probabilistic tsunami amplitudes at the 100m depth contour (as provided by Tsu-DAT). It is noted that accurate estimation of exposure to tsunami will be dependent on the accuracy of the underlying data, in particular the topographic and cadastral information. Since the completion of the Stage 1 assessment, high resolution LiDAR data has been acquired for large portions of the NSW coast and should be used for any future assessment.

Outcomes from the detailed inundation modelling can be used to inform the definition of two aspects of the above approach and to refine the assumptions made as part of the Stage 1 assessment, being; near shore tsunami wave height and tsunami run-up levels. From analysis of the inundation modelling outcomes (see Section 8) it is noted that the vulnerability of a particular site is a product of the following site specific features:-

- Shoaling of the tsunami wave from the 100m water depth (Tsu-DAT location)
- Habitable area below the inundation extent.

Tsunami run-up levels were found to be more a product of nearshore tsunami wave height than any site specific coastline/embayment shape.

Nearshore Shoaling of Tsunami Wave Height

Inspection of the detailed modelling results found that the shoaling coefficient of the tsunami signal from the

100m to similar nearshore water depths varied at each study site and for each recurrence level (or offshore wave height). This suggested that the shoaling of the tsunami signal was not solely dependent on the change in bed level. Multiple regression analysis found that the near shore tsunami wave height is dependent on the water depth (at point of interest), offshore wave height and bed slope. Wave period was not found to be a critical variable.

The relationship is presented in Figure 9.6, which correlates the nearshore wave height (5m water depth) against a function of the average continental shelf slope (between 100m and 5m water depths) and the offshore wave height (100m water depth). The maximum wave height from all scenarios at each ARI level (envelope result) is presented. The observed relationship is estimated as follows:-

$$WH_{20m} = 0.055\left(WH_{100m} \Big/ \tan\beta^{0.8}\right) + 0.2$$

where:-
WH_{20m} = Tsunami Wave Height at 5m water depth
WH_{100m} = Tsunami Wave Height at 100m water depth (taken from Tsu-DAT)
$\tan\beta$ = average continental slope between 100m and 5m water depth

Tsunami Run-up Level

As can be seen from the inundation and hazard mapping (Section 8), the spatial distribution of peak run-up level and the extent of tsunami inundation are highly dependent on local topographic features. A simple measure of the run-up level can be made using the maximum run-up level at a given site. Figure 9.7 presents the maximum run-up level (envelope result at each ARI level) against the maximum near shore crest level (wave height plus tide level at the 5m water depth). The correlation shows a predominantly linear response, which suggests that the influence of coastline/embayment shape (which is distinct for each site) is not a dominant factor in ultimate run-up levels over complex low-lying foreshore areas. Furthermore, the magnitude of maximum run-up is comparable to the magnitude of tsunami wave crest, albeit around 10-30% larger. However, the use of the maximum run-up level would significantly overestimate the total area of inundation (it being an isolated peak level); therefore tsunami wave crest levels at 5m water depth, being more representative of average run-up levels across the study areas, are deemed appropriate for estimating tsunami run-up levels and hence the exposure at a given site.

Count of Cadastral Lots Subject to Inundation

Once the tsunami run-up level is estimated, mapping of the inundation extent at each site can be made and a cadastral count within this inundation extent undertaken. However, the mapping of site specific inundation extents is not trivial and, given the empirical and generalised approach of estimating the run-up level, is not considered to be a valuable exercise. A more generic relationship to provide an estimate of the number of properties vulnerable to inundation has therefore been developed. First, a count of the number of cadastral lots below the 5mAHD contour is made. The total number of lots below 5mAHD is then scaled based on the

estimated tsunami wave run-up level to estimate those subject to inundation, as follows:-

$$Lots_{ARI} = 0.7\left(\frac{WL_{ARI}}{5}\right) \times Lots_{-5mAHD}$$

where:-
$Lots_{ARI}$ is the number of lots inundated at a given recurrence interval
WL_{ARI} is tsunami crest level (mAHD) at 5m water depth for a given recurrence interval
$Lots_{-5mAHD}$ is the total number of lots below 5mAHD

The estimation of cadastral lots subject to inundation using the revised-broad based assessment is provided in Appendix E. To assess the reliability of the revised broad-based approach, the resulting number of lots affected by inundation can be compared to the total number identified by the detailed inundation modelling and hazard mapping (as summarised in Table 9.1). This comparison is presented in Table 9.4 at the 2000-years ARI level, considered an appropriate level to identify particularly vulnerable sites based on inundation thresholds at each of the Stage 2 study sites.

Table 9-5: Comparison of Calculated and Estimated Exposure (by Cadastral Lots at the 2000-years ARI level)

Calculated Exposure (Stage 2 Inundation Modelling)		Estimated Exposure (Modified Broad Based Approach)	
Site	Affected Lots	Site	Affected Lots
2281 - Swansea	2502	2281 - Swansea	2391
2231 - Kurnell	469	2231 - Kurnell	502
2095 - Manly	456	2095 - Manly	431
2230 - Cronulla	573	2230 - Cronulla	229
2548 - Merimbula	300	2548 - Merimbula	272
2500 - Port Kembla	38	2500 - Port Kembla	60
2505 - Wollongong	85	2505 - Wollongong	381
2549 - Pambula	18	2549 - Pambula	19

The comparison shows that the modified assumptions improve the accuracy of the broad based approach with a reasonable match in the counts of exposed lots at most locations (noting that the same high resolution topography data has been used in each instance). More importantly, the relative exposure of each site, or the vulnerability ranking, is well matched.

The exception to this is Wollongong, where the broad based approach significantly overestimates the total exposed lots and increases the relative vulnerability ranking of that location. This is due to the fact that a large number of lots are situated below the 5mAHD level, but are protected by a significant dune system with a crest level of around 7mAHD that inhibits inundation of the area. This indicates that some subjective assessment is required when calculating the number of lots below 5mAHD that are potentially subject to inundation from tsunami.

Despite this, the modified assumptions for the broad based approach are considered suitable for re-assessment of NSW coastal vulnerability to tsunami.

10 CONCLUSIONS AND RECOMMENDATIONS

This report has summarised the methodologies and outcomes from detailed tsunami inundation modelling and deterministic hazard mapping for specific sites along the NSW coast undertaken as part of Stage 2 of the NSW Tsunami Risk Assessment. This study has built upon earlier work undertaken by Risk Frontiers and URS Corporation (2008) as part of Stage 1 of the NSW assessment. Stage 1 was a broad-based risk assessment of the entire NSW coast, with Stage 2 comprising detailed inundation modelling and risk assessment of areas highlighted in Stage 1 as being potentially more vulnerable to tsunami.

The tsunami risk assessment has focused on subduction zone earthquake sources from around the Pacific basin, which account for most tsunami events that affect eastern Australia. Scenarios for other potential sources of tsunami, such as underwater landslides, volcanos and shelf collapses, have not been considered within this assessment. NSW is exposed to tsunami originating from a range of possible sources. There exist a number of subduction zones that border the Pacific Ocean basin, along what is known as the 'Pacific Ring of Fire'. These are considered to provide the most likely threat of tsunami along the NSW coast.

The overall objective of this project was to identify and outline areas of 'high hazard' resulting from potential major tsunami events along the NSW coastline. This will allow for an improved understanding of the tsunami risk to the NSW coastline, enabling future consideration of tsunami impacts in coastal zone management and planning and assist in the development of tsunami emergency planning, response and community education.

Numerical model simulations of selected tsunami scenarios have been undertaken using a calibrated Delft3D model system for five NSW coastal sites and the study has utilised data from the Tsu-DAT and T2 data bases developed by Geoscience Australia and Bureau of Meteorology, respectively. The model system has been demonstrated to reasonably simulate historical tsunami along the NSW coast and replicates the inundation from a benchmark event extremely well.

Selected tsunami scenarios not only allowed for the investigation of events of a range of magnitudes from a range of subduction zone sources, but also at two tide phasings. Tidal phasing, however, was not found to influence the shoaling of the tsunami wave, but does affect the maximum crest level and hence the run-up level of an event. Furthermore, the embayment shape was found to be of little influence to the near shore shoaling and resulting run-up level of tsunami.

It is generally considered that the NSW coast has a medium exposure to tsunami, particularly when compared to other coastlines around Australia and the region. The results from the detailed inundation modelling indicate that tsunami effects along the NSW coast may only be significant at the 1,000 to 2,000-years ARI level (and greater) for subduction zone generated events.

Modelled output is provided as spatial plots (Appendix D) for a range of hydraulic parameters. It is intended that these results enable a detailed risk assessment of each study site and provide for informed emergency management planning and decision making. Results have also been provided to the Bureau of Meteorology for review and assessment of the Joint Australian Tsunami Warning System.

A review of the Stage 1 vulnerability assessment has been completed and refinements to the underlying assumptions of the Stage 1 methodology are proposed. The outcome of this review will allow the broad-

based assessment to be re-visited so that the vulnerability rankings of other sites along the NSW coast can be improved to inform the selection of sites for future detailed inundation modelling campaigns.

The following recommendations are made:-

- Further consideration of other potential sources of tsunami, such as shelf collapse, should be made in order to complete the understanding of tsunami risk along the NSW coast.
- Further investigation of tsunami behaviour within estuarine/coastal river systems is required.
- Re-assess the Stage 1 coastal vulnerability assessment based on the information provided in Section 9 to improve the current vulnerability ranking of NSW coastal sites.

11 LIMITATIONS AND QUALIFICATIONS

This study has involved the detailed numerical modelling of synthetic (hypothetical) tsunami events propagating into complex nearshore and foreshore areas. The reliability and accuracy of the study outcomes are reliant on a range of underlying assumptions and data that have varying degrees of uncertainty. In order to provide context to the findings and outcomes of this study, a summary of the key limitations is provided herein.

11.1 Numerical Model Setup

The numerical model set-up and calibration depends on the quality of data available. The flow regime and processes of foreshore overtopping and inundation are complicated and can only be represented by schematised model layouts. Hence there will be a level of uncertainty in the results and this should be borne in mind in their application.

Model grid resolution was selected on the basis of the available survey data and requirements for describing tsunami propagation and overland flow, while maintaining manageable and practical simulation run times. Typically, the foreshore areas of the study sites are described by a 10m resolution grid with an average land level assigned to each grid point from nearby survey data. Survey data accuracies are detailed in Section 3.

Therefore, some smoothing of the foreshore terrain is tolerated and in line with this, roughness maps are utilised to describe the effective average roughness of different areas such as parkland/bush, residential and road areas. The result is that very small features, for example trees and gutters, are not specifically described in the model, however, such small scale features are not considered to influence the overland propagation of tsunami. Sensitivity testing of the model setup was also undertaken to ensure a robust and practical model setup. The model bathymetry (topography and seabed) was fixed for all modelled scenarios, and hence the potential erosion caused by tsunami overtopping has been disregarded.

Boundary conditions have been derived from numerical modelling undertaken by the Bureau of Meteorology (BoM). Full details of this modelling are contained within BoM (2010) and some assumptions that underlie that modelling exercise are discussed in the Section below.

Model validation was undertaken where possible. This included comparison to benchmark scenarios of tsunami run-up and site-specific modelling of measured events. It should be noted, however, that no site-specific tsunami run-up events have been observed that would allow detailed model calibration.

11.2 Tsunamigenic Sources

NSW is exposed to tsunami originating from a range of possible sources; however, it is considered that the most significant tsunami threat to the NSW coast would be from those originating along the various tectonic subduction zones on the edge of the Indo-Australian Plate, in the South West Pacific. Other potential sources of tsunami that may affect the NSW coast, and include landslides off the continental shelf (Geoscience Australia, 2009), are not addressed in this study. This assumption is considered valid given the overall contribution and likelihood of subduction zone earthquakes to the tsunami hazard along the New South Wales

coast, and the more detailed understanding of their occurrence and magnitude (based on zone dimensions and convergence rates). Furthermore, the focus on subduction zones in the Pacific Ocean is justified because they are known to have produced major historical tsunami and are considered the most likely source of future events along the NSW coastline (BoM, 2010).

Two separate tsunami databases have been developed to describe the risk of subduction zone earthquakes in Australia. They are the Geoscience Australia Tsunami Data Access Tool (Tsu-DAT) and the BoM Enhanced Tsunami Scenario Database: T2 (T2 Database). This study developed a method of utilising both databases for scenario selection and model boundary condition preparation. However, at their core, both databases contain a population of synthetic, hypothetical tsunami events that are based on the current understanding of subduction zone dimensions and seismic activity. It must be noted then that the modelled scenarios will differ from real events and that no two events (even from the same source zone) will be the same.

The rupture models that are used to generate the tsunami events assume a constant scaling law that relates fault length and width to magnitude and also model uniform slip across the fault. In reality such a relationship is unlikely to hold and will be dependent on the regional tectonic features. The approaches of both synthetic databases are therefore simplifications used to model events.

Truly realistic subduction zone ruptures, with variable dimensions and discontinuous and focused slip patches, cannot be comprehensively understood or modelled. The resulting irregularities in the seafloor displacements are likely to lead to greater focussing of tsunami energy along the rupture and potentially lead to larger localised wave heights than what can be achieved in the modelling exercise presented in this study.

11.3 Probability

Recurrence interval estimates identified within this study are based on the recurrence intervals presented in Tsu-DAT. Based on the Probabilistic Tsunami Hazard Analysis (PTHA) for Australia, Tsu-DAT attaches probabilities to every synthetic event in the database. Probabilities are assigned according to a recurrence model that provides a best fit to a global database of subduction zone earthquakes. Full details are described in Burbridge (2008).

A tsunami of a particular recurrence interval at an earthquake epicentre does not necessarily become the equivalent recurrence interval tsunami (in terms of wave height/wave run-up) at any inshore location. Therefore, the recurrence intervals presented in this study are defined based on tsunami magnitudes at the 100m depth contour at each of the study sites, from the Tsu-DAT database.

Tsunami run-up and inundation will be significantly influenced by the orientation of the coastline and the interaction of the incoming tsunami with the near shore region. As such, the resulting inundation from a (say) 500-years ARI tsunami in 100m water depth does not lead necessarily to the 500-years ARI inundation extent on land. To account for this within the current study a series of model runs was completed at each recurrence level (defined by wave height at the 100m water depth) to assess a range of tsunamigenic sources, which provides for a better estimate of the inundation at the recurrence level. Nonetheless, the average recurrence intervals presented can be considered a best estimate only.

Another consideration is the joint occurrence of the tsunami peak and tide level. In reality the peak of a tsunami could occur at any tide level, with those occurring at high tide presumably posing greater hazard. However, the true joint occurrence of tide and tsunami would be very site dependant and the historical record is insufficient to make any meaningful estimate. This study has therefore adopted the HAT tide level at each site. It should be noted that while this seems conservative, non-astronomic contributors to coastal water levels (such as meteorological effects) result in this tide level being reached or exceeded several times a year. Furthermore, tsunami waves persist for some hours and would most likely encounter a high tide, even if not at a time of the highest tsunami peaks.

11.4 General

The investigation and modelling procedures adopted for this study follow industry standards and considerable care has been applied to the preparation of the results. Overall, best engineering practice was applied and the outcomes and findings of this study should be adopted in the context of the above limitations.

Study results should not be used for purposes other than those for which they were prepared.

12 ACKNOWLEDGEMENTS

Many thanks are required for the various members of *Tsunami Inundation Modelling and Risk Assessment Steering Committee*. Simon Opper, Felicia Andrews, Belinda Davies and Michelle Bouvet of the NSW SES are thanked for their contribution of data and other inputs, as well as their valuable review and input to the report. David Hanslow and Ainslie Frazer of NSW OEH are thanked for their involvement in steering the project approach and methodology, as well as the technical review. Diana Greenslade and the Australia BoM are thanked for their contribution of the T2 database and their involvement in the model validation component and technical review. Nick Horspool and GA are thanked for their contribution of Tsu-DAT and other geotechnical information, as well guidance in scenario selection and model validation.

Funding was provided through the National Disaster Mitigation Program.

13 REFERENCES

Baldock, T., Barnes, M., Guard, P. and Hie, T. (2008). *Modelling of the Potential Nearshore Modification of Tsunami Waves Within Typical Coastal Settings along the NSW Coast..* Coastal Engineering Research Centre, University of Queensland.

Beccari, B (2009). *Measurements and Impacts of the Chilean Tsunami of May 1960 in New South Wales, Australia*. NSW SES Report 08/0576.

Beccari, B., Davies, B (2009). *Tsunami in NSW – The Chilean Waves of 1960*. NSW Coastal Conference, Ballina, November 2009.

Burbidge, D., Cummins, P., Mleczko, R., Thio, H.K (2008). *A Probabilistic Tsunami Hazard Assessment for Western Australia.* Pure and Applied Geophysics, 165, pp: 2059-2088.

Burbidge, D (2010). *Tsunami Hazard in the Australian region*. Australian Meteorology and Oceanographic Society 17th Annual Conference, Canberra, January 2010.

Bureau of Meteorology and the Centre for Earthquake Research in Australia (1998). *Contemporary Assessment of Tsunami Risk and Implications for early warnings for Australia and its Island Territories*, Project 11/94.

Bureau of Meteorology (2010). *Tsunami Emergency Planning in Australia*. Australian Emergency Manual Series, Manual 46.

Deltares (2010). *Delft3D-FLOW – User Manual*. Version 3.14, Revision 12556. Deltares, Rotterdam.

Dominy-Howes, D. (2007). *Geological and Historical Records of Tsunami in Australia.* Marine Geology, 239, pp: 99-123.

Egbert, G., Erofeeva, S (2002). *Efficient Inverse Modelling of Barotropic Ocean Tides.* Journal of Atmospheric and Oceanic Technology, 19, 2, pp: 183-204.

Gayer, G., Leschka, S., Nöhren, I., Larsen, O., Günther, G. (2010). *Tsunami inundation modelling based on detailed roughness maps of densely populated areas*. Nat. Hazards Earth Syst. Sci., 10, 1679–1687, 2010.

Geoscience Australia (2009). *Revealing the Continential Shelf off the NSW Coast*. AUSGEO News. Issue 89. March 2009. http://www.ga.gov.au/image_cache/GA11088.pdf

Geoscience Australia (2010a). *Tsunami Hazard – What Causes Tsunami*. Geoscience Australia website. http://www.ga.gov.au/hazards/tsunami/tsunami-basics/causes.html.

Geoscience Australia (2010b). *Tsunami Data Access Tool (Tsu-DAT) - User Guide, Version 1.0*. Geoscience Australia and the Attorney-General's Department. GeoCat No. 70539. 2010.Greenslade, D., A., Allen, S, Simanjuntak (2011). *An Evaluation of Tsunami Forecasts from the T2 Scenario Database.* Pure and Applied Geophysics, Volume 168, Issue 6-7, pp. 1137-1151.

Greenslade, D., Annunziato, A., Babeyko, A., Burbidge, D., Ellguth, E., Horspool, N., Kumar, T.S., Kumar, C.H.P., Moore, C., Rakowsky, N., Riedlinger, T., Ruangrassamee, A., Srivihok, P., Titov, V (2010). *A Preliminary Analysis of the Diversity in Scenario-based Tsunami Forecasts in the Indian Ocean.* Proceedings of the Indian Ocean Tsunami Modelling Symposium, Fremantle, Western Australia, 12-15 October 2010.

Greenslade, D., Simanjuntak, A., Allen, S (2009). *An Enhanced Tsunami Scenario Database: T2.* CAWCR Technical Report No. 014. The Centre for Australian Weather and Climate Research. Bureau of Meteorology.

Greenslade, D., Titov, V.V (2008). *A Comparison Study of Two Numerical Tsunami Forecasting Systems*. Pure and Applied Geophysics, 165, pp: 1991-2001.

IOC-UNESCO (1998). *Post-Tsunami Survey Field Guide, 1st edition*. IOC Manuals and Guides, Intergovernmental Oceanographic Commission.

Kamphuis, J., W (2010). *Introduction to Coastal Engineering and Management*. 2nd Edition. World Scientific Advanced Series on Ocean Engineering – Volume 30.

Matsuyama, M., Tanaka, H (2001). *An Experimental Study of the Highest Run-Up Height in the 1993 Hokkaido Nansei-Oki Earthquake Tsunami.* ITS 2001 Proceedings, Session 7, Number 7-21, pp: 879

NOAA (2007). *Standards, Criteria and Procedures for NOAA – Evaluation of Tsunami Numerical Models*. NOAA Technical Memorandum OAR PMEL-135. National Oceanic and Atmospheric Administration. Pacific Marine Environmental Laboratory, Seattle, WA. May 2007.

National Tide Tables (2010). *Australian Hydro-graphic Publication 11*. Department of Defence, Commonwealth of Australia.

Neilson, O., Roberts, S., Gray, D., McPherson, A., Hitchman, A (2005). *Hydrodynamic modelling of coastal inundation*. Geoscience Australia.

Risk Frontiers and URS Corporation (2008). *Development of Information for a Risk Assessment of the NSW Coast.* Report prepared for New South Wales Department of Environment, Climate Change and Water and New South Wales State Emergency Service.

State Emergency Service (2008). *Tsunami Emergency Management Sub Plan – A Sub Plan of the NSW Disaster Plan (Displan)*, NSW State Emergency Service, Wollongong.

Somerville, P., Hanslow, D.J. and Gissing, A (2009). *NSW Tsunami Risk – An Overview of the NSW Risk Assessment Scoping Study*. Joint NSW and Victorian Flood Management Conference. Albury-Wodonga, February 2009.

Stelling, G. S (1984). *On the construction of computational methods for shallow water flow problems*. Tech. Rep. 35, Rijkswaterstaat. pp: 94, 216, 282, 286, 287, 288, 289, 292, 293, 295, 306, 383, 384, 536.

Stelling, G. S., Duinmeijer, S (2003). *A staggered conservative scheme for every Froude number in rapidly varied shallow water flows*." International Journal Numerical Methods In Fluids 43: 1329-1354. pp: 94, 287, 293, 307.

Synolakis, C.E., Bernard, E.N., Titov, V.V., Kanoglu, U., Gonzalez, F.I (2008). *Validation and Verification of Numerical Tsunami Models.* Pure and Applied Geophysics, 165, pp: 2197-2228.

Takahashi, T., Shuto, N (1994). Study of the *1993 Hokkaido Nansei-Oki Earthquake Tsunami by Computation.* Proceedings of Earth 1994 in Japan, F31-06, 1995. (In Japanese).

Tenix (2008). *Marine LiDAR survey data and spatial modelling products of NSW Central Coast*. Report of Survey. CLPT-6544-001-08. 29 August 2008.

Thio, H.K., Sommerille, P. (2006). *Probabilistic Tsunami Hazard Analysis for Australia.* Unpublished Report.

Uslu, B. and Greenslade, D. (2012). *Validation of Tsunami Warning Thresholds using Inundation Modelling*. Australian Oceanographic and Meteorological Society Annual Conference, Sydney, February 2012.

Whiteway, T. (2009). *Australian Bathymetry and Topography Grid*. Geoscience Australia.

Wilkinson, F. (2005). *Coastal Design and Tsunami Mitigation for Shelter/House Reconstruction on the West Coast Aceh*. International Symposium Disaster Reduction on Coasts. Monash University, Melbourne, 14 – 16 November 2005.

Zhang, H., Shi, Y., Yuen, D., Yan, Z., Yuan, X., Zhang, C. (2008). *Modelling and Visualization of Tsunamis*. Pure and Applied Geophysics, 165, pp: 475-496.